

Fluorescent Pirenzepine Derivatives as Potential Bitopic Ligands of the Human M1 Muscarinic Receptor

Chouaib Tahtaoui,^{†,‡} Isabelle Parrot,^{†,§} Philippe Klotz,[†] Fabrice Guillier,^{†,||} Jean-Luc Galzi,^{||} Marcel Hibert,[†] and Brigitte Ilien^{*,||}

Laboratoire de Pharmacochimie de la Communication Cellulaire, Faculté de Pharmacie, UMR CNRS/ULP 7081, IFR 85, 74 route du Rhin, BP 10413, 67412 Illkirch, France, and Département Récepteurs et Protéines Membranaires, CNRS UPR 9050, ESBS, IFR 85, Boulevard Sébastien Brant, BP 10413, 67412 Illkirch, France

Received March 1, 2004

Following a recent description of fluorescence resonance energy transfer between enhanced green fluorescent protein (EGFP)-fused human muscarinic M1 receptors and Bodipy-labeled pirenzepine, we synthesized seven fluorescent derivatives of this antagonist in order to further characterize ligand–receptor interactions. These compounds carry Bodipy [558/568], Rhodamine Red-X [560/580], or Fluorolink Cy3 [550/570] fluorophores connected to pirenzepine through various linkers. All molecules reversibly bind with high affinity to M1 receptors (radioligand and energy transfer binding experiments) provided that the linker contains more than six atoms. The energy transfer efficiency exhibits modest variations among ligands, indicating that the distance separating EGFP from the fluorophores remains almost constant. This also supports the notion that the fluorophores may bind to the receptor protein. Kinetic analyses reveal that the dissociation of two Bodipy derivatives (10 or 12 atom long linkers) is sensitive to the presence of the allosteric modulator brucine, while that of all other molecules (15–24 atom long linkers) is not. The data favor the idea that these analogues might interact with both the acetylcholine and the brucine binding domains.

Introduction

Fluorescence resonance energy transfer (FRET) between a fluorescent donor–acceptor pair is a powerful method to investigate intra- and intermolecular association processes.^{1,2} Although energy transfer can be recorded using the intrinsic fluorescence of a receptor protein (Trp³ or unnatural amino acids⁴) or fluorescent antibodies⁵ as energy donors together with a fluorescent ligand taken as the acceptor, receptor–ligand interactions are more easily followed, in real-time and on living cells, using enhanced green fluorescent protein (EGFP)-fused receptors as the donor species.

On tachykinin NK2 and chemokine CXCR4 receptors, we have shown that time monitoring of EGFP fluorescence extinction, due to ligand binding, allows us (i) to determine equilibrium and kinetic parameters of the interaction, (ii) to reveal different interconverting receptor states, and (iii) to precisely identify the relationship between agonist-induced conformational changes and functional states of the receptor.^{6–9} When combined with cell imaging, further information on receptor subcellular trafficking can be acquired.

Various fluorescent muscarinic antagonists such as anthrolycholine¹⁰ or telenzepine bearing fluorophores such as Eosin-5 [519/540], Fluorescein [490/514], or

Cascade Blue [396/410] dyes,^{11,12} as well as pirenzepine labeled with Bodipy FL [504/511]¹³ or with Bodipy [558/568], were presented as alternatives to radiotracers or used to examine muscarinic M1 receptor tissue distribution. Because Bodipy [558/568]-pirenzepine [here referred to as Bo(10)PZ] derives from the well-known high affinity muscarinic M1 antagonist and displays almost ideal spectroscopic properties for an energy acceptor of excited EGFP, it has been selected to study the molecular interactions with the human M1 muscarinic receptor.¹⁴ High efficiency for energy transfer from an EGFP-fused hM1 receptor to Bo(10)PZ was detected through shortening of the receptor N-tail [EGFP(Δ17)-hM1 chimera], without detectable consequences on drug recognition or functional properties of the receptor.¹⁴ This work also provided structural information on the folding of the receptor N terminus and led to the description of a miniaturized FRET-based assay for drug discovery.

FRET efficiency depends on the extent of spectral overlap between donor emission and acceptor absorbance, the relative orientation of the donor and acceptor transition dipoles, and the distance separating both fluorophores.¹⁵ In an attempt to further optimize the sensitivity of the M1 FRET assay, we synthesized a series of new fluorescent derivatives of pirenzepine, all endowed with acceptor properties for energy transfer from excited EGFP. Three fluorophores (Bodipy [558/568], Rhodamine Red-X[560/580], and Fluorolink Cy3 [550/570]), exhibiting distinct spectroscopic properties, were linked to pirenzepine via spacers differing in length and chemical nature.

The ligand binding affinity was assessed, at equilibrium, through conventional [³H]QNB competition ex-

* To whom correspondence should be addressed. Tel: 00 33(0)3 90 24 47 38. Fax: 00 33(0)3 90 24 48 29. E-mail: ilien@esbs.u-strasbg.fr.

[†] UMR CNRS/ULP 7081.

[‡] Present address: Arpida AG, Research & Development of Anti-Infectives, Dammstrasse 36, CH-4142 Muenchenstein, Switzerland.

[§] Present address: LAPP, UMR 5810, Université de Montpellier, 2, Place Eugène Bataillon, 34095 Montpellier Cedex 5, France.

^{||} Present address: Laboratoires Fournier S.A., Département Chimie-USP, 50, rue de Dijon, 21121 Daix, France.

^{||} CNRS UPR 9050.

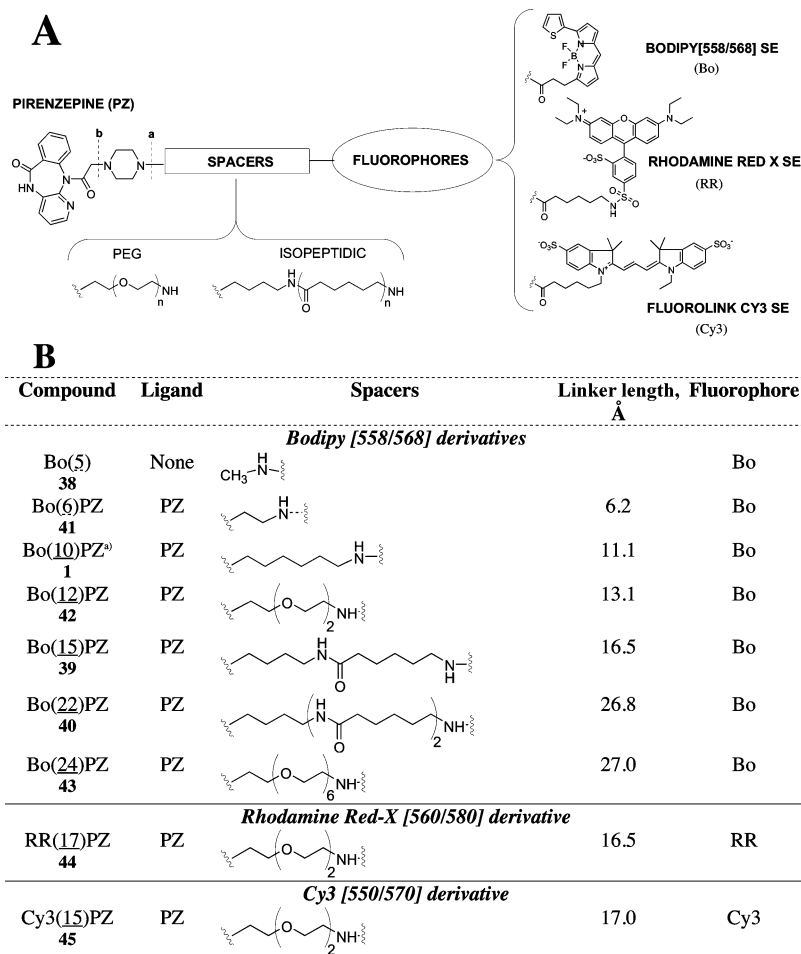


Figure 1. Chemical structures of the fluorescent derivatives. (A) General template for fluorescent pirenzepine derivatives. Pirenzepine was connected through various spacers of PEG or isopeptidic type to succinimidyl esters (SE) of Bodipy [558/568] (Bo, Molecular Probes), Rhodamine Red-X [560/580] (RR, Molecular Probes), or Fluorolink Cy3 [550/570] (Cy3, Amersham Pharmacia Biotech). The spectroscopic characteristics of the various fluorophores are given in Table 1. (B) Overview of chemical structures of the various fluorescent derivatives. The compounds are defined by three terms, i.e., PZ (for pirenzepine), an underlined number indicating the total number of atoms, including those of the spacer separating pirenzepine from the fluorophore, and the abbreviated fluorophore name. Full linker lengths (Å), in an extended configuration, were obtained through Chem3D calculation after energy minimization. The correspondence with the final products obtained throughout the syntheses is given below each name (bold characters). (a) Bo(10)PZ, referred to as product **1**, was purchased from Molecular Probes.

periments and through FRET assays using the EGFP-(Δ17)hM1 chimera. The determination of maximal fluorescence extinction at saturating concentrations of ligand allowed us to calculate energy transfer efficiencies and to estimate mean distances separating EGFP from each receptor-bound fluorophore. Finally, dissociation kinetics of the different fluorescent ligands from M1 receptors, and their alteration by the allosteric modulator brucine,^{16,17} were followed in real-time through FRET.

Results and Discussion

A set of nine fluorescent donor–acceptor pairs have been designed, characterized, and compared for optimal binding and FRET efficiency at EGFP-fused muscarinic M1 receptors. Several fluorescent ligands have been synthesized by linking the distal piperazinyl nitrogen of pirenzepine to three types of fluorophores through various functionalized spacers (Figure 1).

Choice and Characterization of Donor–Acceptor Fluorescent Pairs. Pirenzepine was selected as the prototypic ligand since (i) it is a well-known high affinity M1 muscarinic antagonist, (ii) its derivatization

by several side chains has been extensively studied in terms of binding affinity and selectivity,¹⁸ and (iii) its Bodipy [558/568] derivative, which is commercially available and is here referred to as Bo(10)PZ or compound **1**, has been recently characterized as an appropriate acceptor partner for efficient energy transfer from EGFP-fused human M1 receptors.¹⁴ Bodipy [558/568] was taken here as the fluorophore of reference to compare binding properties and FRET efficiencies of a series of pirenzepine derivatives differing by the nature [isopeptidic or poly(ethylene glycol) (PEG)-like] and the length (5–24 atoms) of the linker and by the fluorophore moiety (Bodipy, Rhodamine Red-X, or Cy3) (Figure 1).

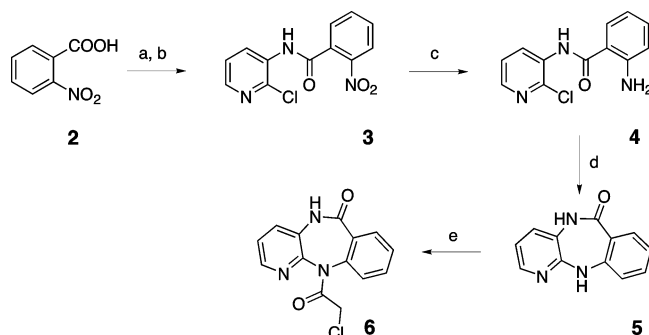
The three selected fluorescent dyes are endowed with the appropriate spectroscopic properties expected for an energy acceptor from excited EGFP (Table 1). Indeed, they display negligible absorbance at the EGFP excitation wavelength (470–480 nm), negligible emission at EGFP's emission wavelength (510 nm), appreciable overlap of their absorbance spectra with the emission spectrum of EGFP, and large molecular extinction coefficients. The last two properties, especially evident for the Cy3 derivative, are responsible for the substan-

Table 1. Spectroscopic Parameters of Fluorophores and of Their Pirenzepine Derivatives^a

molecule	absorption				fluorescence				
	MeOH		buffer		MeOH	buffer	donor/acceptor pair		
	$\epsilon \times 10^{+3}$ (M ⁻¹ cm ⁻¹)	λ_{\max} (nm)	$\epsilon \times 10^{+3}$ (M ⁻¹ cm ⁻¹)	λ_{\max} (nm)	λ_{\max} emission (nm)	λ_{\max} emission (nm)	spectral overlap (cm ³ M ⁻¹) $\times 10^{-13}$	Förster radius (Å)	
Bodipy [558/568] SE ^a	97	558			568				
Bo derivatives	75	559–561	61	562–567	ND	570–575	1.48 \pm 0.03 (<i>n</i> = 6)	49.6 \pm 0.2 (<i>n</i> = 6)	
Rhodamine Red-X SE ^a	129	560			580				
RR derivative	88	560	83	570	ND	590	1.87 \pm 0.11 (<i>n</i> = 6)	51.5 \pm 0.5 (<i>n</i> = 6)	
Fluorolink Cy3 SE ^b	150	550			570				
Cy3 derivative		553	152	551	ND	564	5.2 \pm 0.2 (<i>n</i> = 6)	61.2 \pm 0.4 (<i>n</i> = 6)	

^a Values for succinimidyl esters are from Molecular Probes. ^b Values for succinimidyl esters are from Amersham Pharmacia Biotech. Spectroscopic parameters are determined in MeOH or in Hepes–BSA buffer. The spectral overlap integral for the combined donor emission and acceptor absorbance as well as the Förster radius R_0 are from measurements in Hepes–BSA buffer and calculated as reported in the Experimental Section.

Scheme 1. Synthesis of the *N*-Chloroacetyl-benzodiazepinone **6**^a



^a Legend: (a) (COCl)₂, DMF, THF. (b) 2-Chloro-3-amino pyridine, THF, pyridine, 67% (a + b). (c) SnCl₂, HCl, 86%. (d) 210 °C, 5 min, 80%. (e) Chloroacetyl chloride, Et₃N, dioxane, 70%.

tial spectral overlap integral (J value) with EGFP and for Förster radius (R_0) values in the 50–60 Å range.^{1,15} Data listed in Table 1 also show that spectroscopic parameters of the compounds are moderately sensitive to the environment (methanol vs Hepes buffer) or to chemical derivatization.

Chemistry. The general structure of the probes shown in Figure 1A is obtained by substituting the *N*-methyl group of the piperazine moiety of pirenzepine by various spacer arms so that the pirenzepine core remains unchanged in all probes. To have access to a variety of spacer lengths of different chemical natures, we used PEG type and “isopeptidic” type spacers. Indeed, the nature of the linker might not be neutral in terms of folding and/or ligand interactions with the receptor protein and could thus affect FRET efficiency. In this way, we have developed a chemical strategy to synthesize PEG and isopeptidic spacers of defined lengths and to functionalize them in order to establish the connection between the pirenzepine and a given fluorophore.

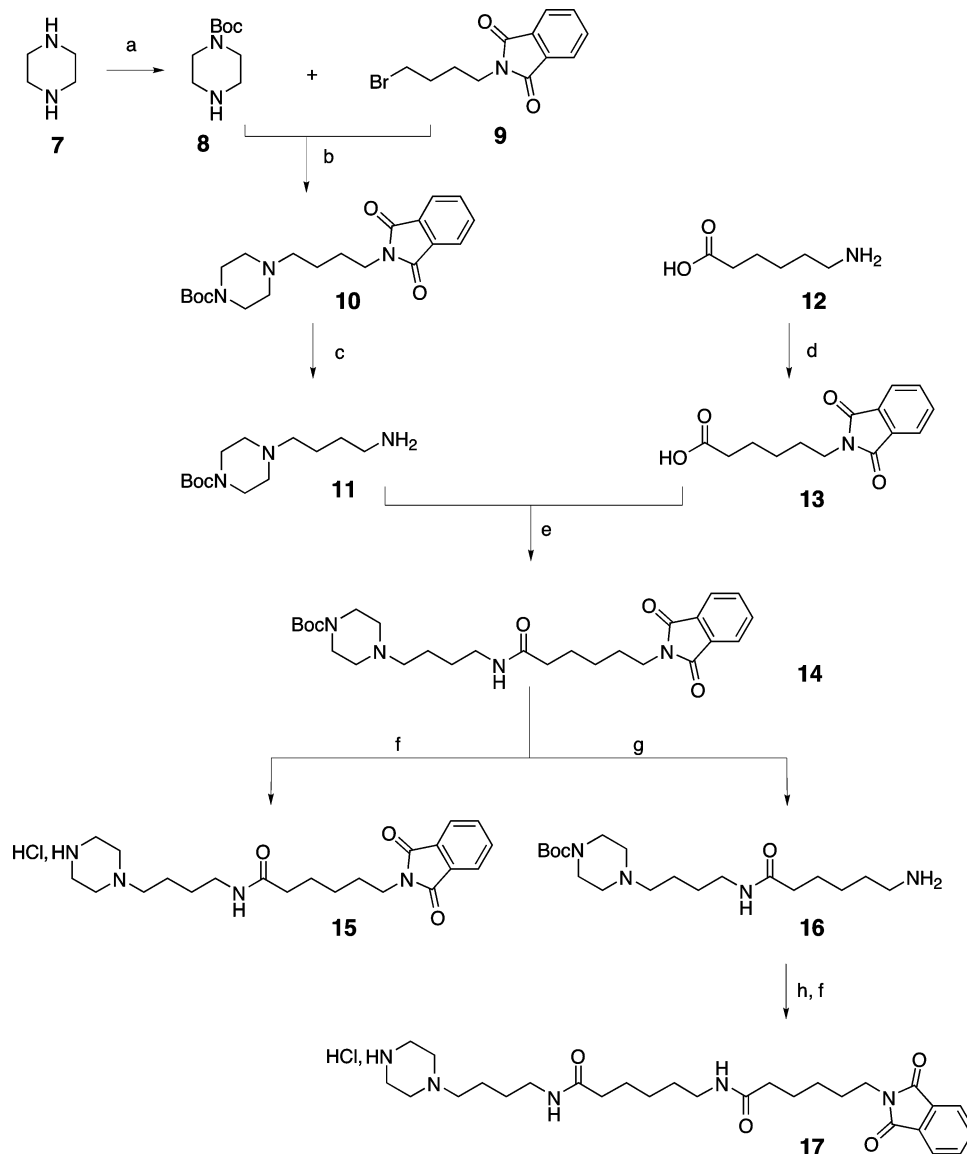
We first attempted to link *N*-demethylated pirenzepine to the spacer through an “a type” disconnection (see Figure 1A). We found that nucleophilic displacement of a mesylate or a bromine from the spacer by the secondary piperazine amine either failed or gave poor yields of the final product. On the other hand, a “b type” disconnection was a much more efficient pathway. Thus, the chloroacetyl-pirenzepine derivative **6** (Scheme 1) could be coupled with the different piperazine spacer molecules.

To connect the spacer with the commercially available succinimidyl esters of the fluorescent Bodipy [558/568], Rhodamine Red-X [560/580], and Fluorolink Cy3 [550/570] molecules, a primary amine was introduced on the opposite extremity of the spacer.

N-Chloroacetyl-benzodiazepinone **6** was obtained as described in Scheme 1.^{19,20} First, 2-nitrobenzoic acid **2** was activated with oxalyl chloride and condensed with 3-amino-2-chloropyridine to give the nitrobenzamide derivative **3**. The nitro group was reduced with stannous chloride to give the aminobenzamide **4** in 86% yield. The benzodiazepinone **5** was then obtained by solvent free intramolecular cyclization of intermediate **4** at 210 °C. We also tried, with poor success (less than 20% yield), to obtain compound **5** from the intermediate **4** according to a “carbon–nitrogen Buchwald–Hartwig” reaction²¹ with Pd(OAc)₂ as the catalyst and *t*-BuOK in toluene. Finally, the diazepinoic compound **5** was *N*-chloroacetylated to give compound **6** with 70% yield.

The isopeptidic spacers **15** and **17** (Scheme 2) were synthesized in a conventional protection–deprotection peptide-like synthesis. The coupling of *N*-Boc piperazine **8** with 4-bromophthalimide **9** in basic conditions gave the protected compound **10**. Deprotection of the phthalimide appendage with ethanolic hydrazine gave the *N*-Boc piperazine aminobutyl molecule **11**, which was coupled with the 6-phthalimidocaproic acid **13** to obtain the first protected spacer **14**. Deprotection of the Boc group with HCl gave the spacer **15** in quantitative yield. To elongate the spacer by one caproic acid unit, the strategy followed for molecule **15** was used again starting from the Boc-protected spacer **14**. Deprotection of the phthalimido group with hydrazine and coupling of the obtained amine **16** with 6-phthalimido caproic acid **13** gave, after Boc deprotection, the second isopeptidic spacer **17** in good yield.

For the PEG spacers (Scheme 3), we developed a strategy that allows the choice of their length and of their α and ω functional groups, as mentioned above. In our particular case, we have placed the piperazine molecule in the α -position and the amine function (masked as an azido group) in the ω -position. For the shortest spacer, **21**, the synthesis started with mesylation of ethylene glycol (EG) at both α - and ω -positions to give the bis-mesylate molecule **19**. One of the mesyl groups was then displaced by sodium azide (**20**), and the other one was substituted with *N*-Boc piperazine **8**,

Scheme 2. Synthesis of the Isopeptidic Piperazine Spacers **15** and **17**^a

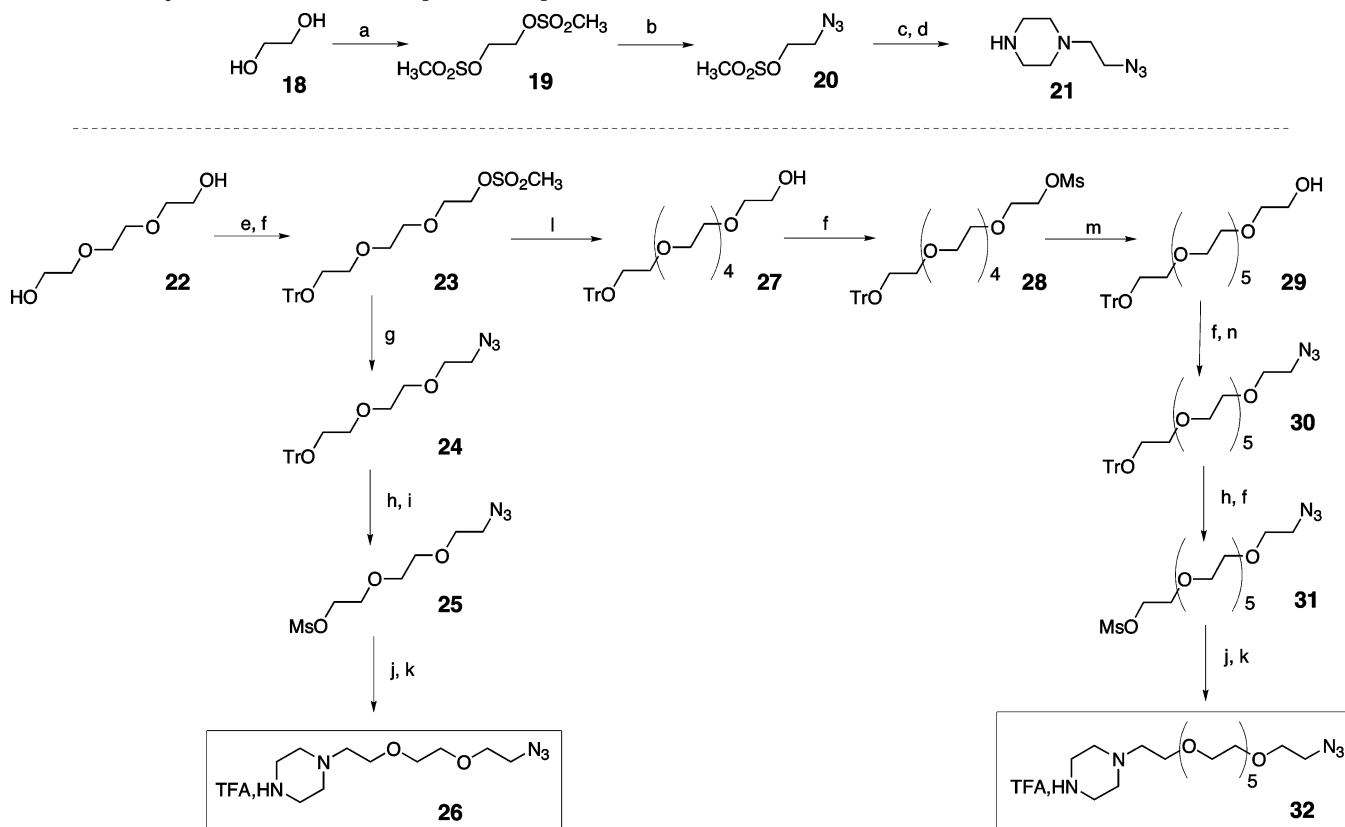
^a Legend: (a) (Boc)₂O, CH₂Cl₂, 75%. (b) DIPEA, CH₃CN, reflux, 95%. (c) H₂N-NH₂, EtOH, reflux, 100% crude. (d) Na₂CO₃, H₂O, *N*-carboxyphthalimide, 70%. (e) DCC, HOBt, NMM, THF, 90%. (f) HCl gaz, quantitative yield. (g) H₂N-NH₂, EtOH, reflux, 100% crude. (h) Compound **13**, DCC, HOBt, NMM, THF, 80%.

to give the shortest spacer **21** in good yields, after Boc deprotection.

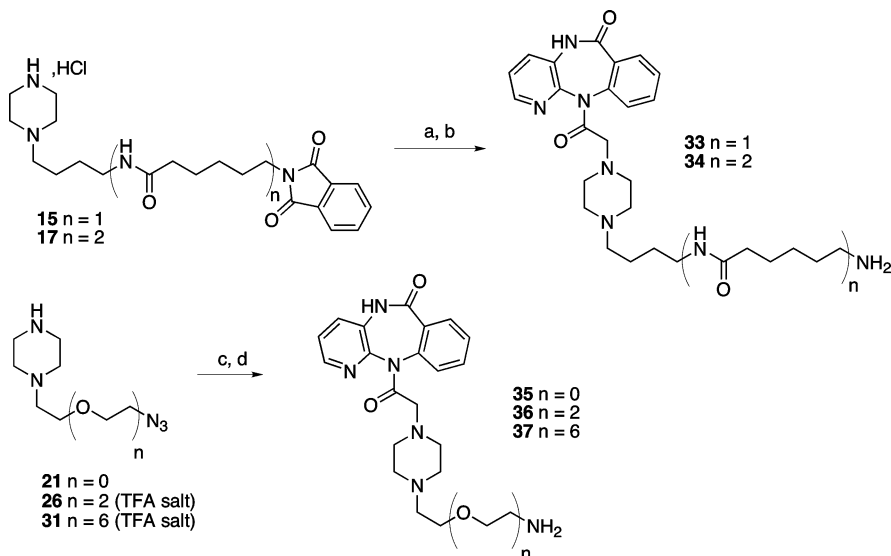
The two other spacers that we used, one of a medium size (**26**; three EG units) and one of a larger size (**32**; seven EG units), were obtained starting from triethylene glycol (TEG) **22** (Scheme 3). Monoprotection of **22** with the trityl group followed by mesylation of the opposite hydroxyl group led to compound **23**, a precursor for spacers **26** and **32**. To obtain spacer **26**, the mesylate group of **23** was displaced by sodium azide to give the azido-trityl TEG compound **24**. The trityl group was then removed by action of TsOH in methanol, and the free alcohol was activated as a mesylate derivative **25**. Nucleophilic displacement with *N*-Boc piperazine **8** gave, after Boc deprotection, the medium spacer **26**. To obtain the "large size" spacer **32**, molecule **23** can be used to add EG, diethylene glycol, or TEG units. In our case, molecule **23** was first coupled to TEG by a "Williamson type" reaction,²² using *t*-BuOK in *t*-BuOH. The obtained elongated PEG **27** was mesylated, and a

second Williamson type coupling reaction with EG was achieved to give the molecule **29** with seven EG units. The functionalization of **29** follows the way that we used for spacer **26**. Activation of the terminal alcohol by a mesylate group and displacement by sodium azide give compound **30**. The trityl protecting group is then removed and replaced by a mesylate one. The resulting compound **31** is subsequently substituted by *N*-Boc piperazine **8** to give the large size spacer **32** in good overall yield.

The three PEG (**21**, **26**, and **32**) as well as the isopeptidic (**15** and **17**) spacers were coupled to the chloroacetylbenzodiazepinone **6** under basic conditions. Isopeptidic spacers were directly coupled to **6** in a mixture of dimethyl sulfoxide (DMSO) and dimethylformamide (DMF) using DIPEA as the base (Scheme 4). The *N*-terminal amine was restored by the action of hydrazine on the phthalimido protecting group to yield molecules **33** and **34**. The PEG spacers were linked to benzodiazepinone **6** in acetonitrile using K₂CO₃ as the

Scheme 3. Synthesis of the PEG Piperazine Spacers **21**, **26**, and **32**^a

^a Legend: (a) MsCl, Et₃N, CH₂Cl₂, 96%. (b) NaN₃, CH₃CN, reflux, 46%. (c) Compound **8**, Et₃N, CH₃CN, reflux, 95%. (d) TFA 50%, CH₂Cl₂, 70%. (e) TrOH, APTS, PhH, reflux. (f) MsCl, Et₃N, CH₂Cl₂, 82% (e + f, **23**), 97% (**28**), 81% (**30**), 84% (h + f, **31**). (g) NaN₃, CH₃CN, reflux, 84%. (h) APTS, MeOH, reflux. (i) MsCl, Et₃N, CH₂Cl₂, 72% (h + i). (j) **8**, Et₃N, CH₃CN, reflux. (k) TFA, 50% CH₂Cl₂, 56% (j + k, **26**), 98% (j + k, **32**). (l) Compound **22**, t-BuOK, t-BuOH, reflux, 82%. (m) Compound **18**, t-BuOK, t-BuOH, 94%. (n) NaN₃, CH₃CN, reflux, 80%.

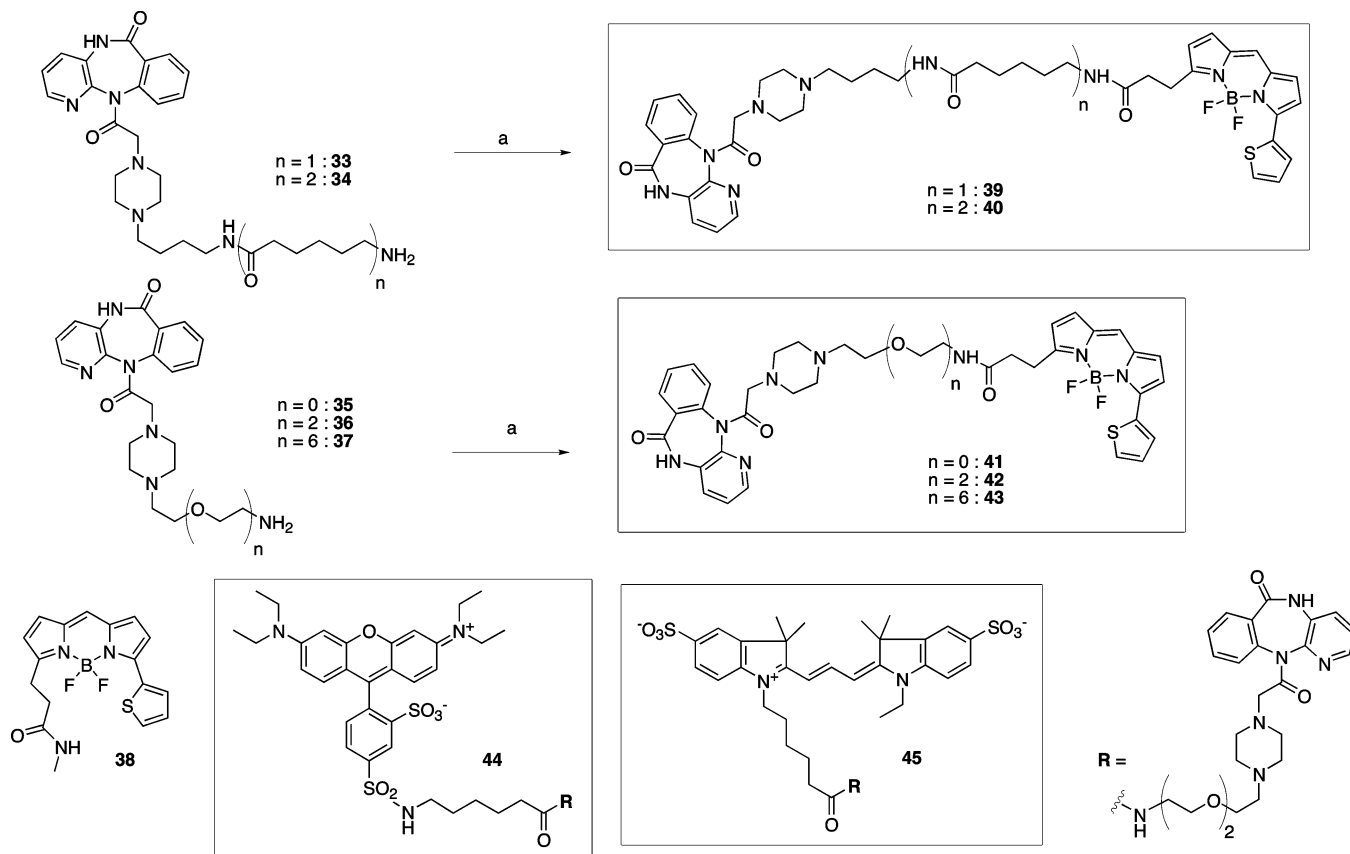
Scheme 4. Linkage of the Spacers to the Pirenzepine Moiety^a

^a Legend: (a) Compound **6**, DIPEA, DMF/DMSO 1/1, reflux. (b) H₂N-NH₂, EtOH, reflux 80% (a + b, **33**), 40% (a + b, **34**). (c) Compound **6**, K₂CO₃, CH₃CN, reflux, 50% (**35**), 82% (**36**), 96% (**37**). (d) PPh₃, H₂O, THF, room temperature, 80% (**35**), 98% (**36**), 76% (**37**).

base. The obtained adducts were then reduced using triphenylphosphine to generate the free terminal amino group present in compounds **35**–**37**.

These five pirenzepine spacer derivatives were finally coupled to commercially available succinimidyl esters of Bodipy [558/568], Rhodamine Red-X [560/580], and Cy3 [550/570] (Scheme 5). The coupling reaction was

performed on micromole amounts of the reagents under basic conditions (see Experimental Section). After high-performance liquid chromatography (HPLC) purification, the expected molecules were analyzed by matrix-assisted laser desorption/ionization time-of-flight (MALDI-TOF) spectrometry. Finally, Bodipy-SE was also coupled to methylamine to give Bo(5), which was

Scheme 5. Synthesis of the Final Fluorescent Probes^a

prepared in order to evaluate the affinity of the Bodipy core alone for the muscarinic M1 receptor. Figure 1B depicts all of the prepared molecules.

Binding Properties of the Fluorescent Ligands at EGFP-Fused M1 Receptors. The interactions of the pirenzepine derivatives with M1 receptors were examined on HEK cells expressing the EGFP(Δ 17)hM1 fluorescent chimera (600 fmoles per 10^6 cells). Figure 2 illustrates, using RR(17)PZ, the set of experiments, which was systematically carried out to characterize ligand binding, i.e., the ability of the fluorescent compound to decrease, in a time, concentration, and atropine sensitive manner, EGFP fluorescence emission.

Upon addition of RR(17)PZ (500 nM) to EGFP(Δ 17)-hM1 cells (Figure 2A, trace a), the fluorescence decreases over time and reaches a plateau after about 20 min (extinction of 55% of total fluorescence), reflecting the association and binding at equilibrium. Normalization of the association trace (a) between 0 and 1 and its presentation on a logarithmic scale as a function of time (Figure 2A, inset) clearly indicate that the RR(17)PZ association proceeds in a multistep complex bimolecular interaction rather than a simple bimolecular interaction. A slow association phase (apparent association velocity constant $k_{app} = 0.004 \text{ s}^{-1}$), accounting for about 20% of RR(17)PZ binding at equilibrium, follows an initial rapid binding component ($k_{app} = 0.0285 \text{ s}^{-1}$). Thus, in contrast with monoexponential fitting of the trace ($k_{app} = 0.0157 \text{ s}^{-1}$), the association of RR(17)PZ is fully and correctly described by a two-exponential decay of fluorescence, i.e., by the occurrence of a fast ($75.4 \pm 2.9\%$ of the FRET signal; $k_{app} = 0.0290 \pm 0.0008 \text{ s}^{-1}$) and of a slow (24.6

$\pm 2.9\%$ of the FRET signal; $k_{app} = 0.0035 \pm 0.0009 \text{ s}^{-1}$) binding component [mean values \pm standard error (SE) for five independent experiments].

When atropine (5 μM) is added before the fluorescent ligand, the binding of RR(17)PZ is fully inhibited (trace b). The fluorescence remains unchanged and perfectly stable over a 2 h period of time, indicating that cell settling or EGFP photobleaching do not occur and are not responsible for the slow association process of the ligand.

When added at RR(17)PZ binding equilibrium (Figure 2A), atropine induces a slow recovery in fluorescence (trace c), reflecting the RR(17)PZ dissociation from the receptor. This process corresponds to a monoexponential recovery of fluorescence and takes place with an off-rate constant of 0.00053 s^{-1} . Four independent experiments, performed under identical conditions, lead to a mean k_{off} value for RR(17)PZ binding of $6.0 \pm 0.3 \cdot 10^{-4} \text{ s}^{-1}$ (Table 3).

Real-time recordings of EGFP(Δ 17)hM1 emission intensity vs RR(17)PZ concentration (Figure 2B) show that fluorescence extinction rates and amplitudes increase with RR(17)PZ concentration and that saturation is obtained around 500 nM. The binding equilibrium is reached at each ligand concentration, provided that the incubation time is long enough. This has been verified by comparing maximal FRET amplitudes measured at time 2000 s with those calculated from two-exponential fitting of the experimental traces, i.e., amplitudes at infinite incubation times (Figure 2C). In some experiments, a linear drift could be detected (slope = -0.002 s^{-1}) in the association process (Figure 2B); this drift was

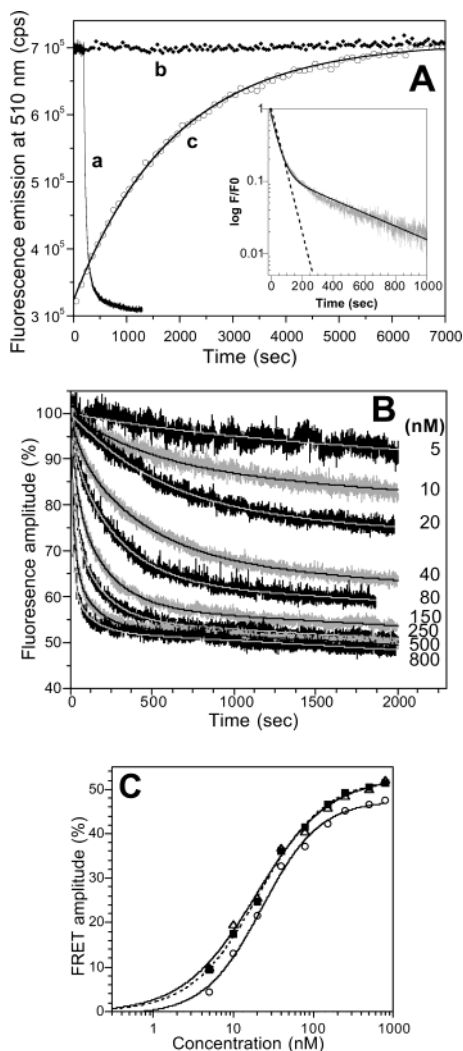


Figure 2. FRET monitoring of RR(17)PZ binding to EGFP-(Δ 17)hM1 receptors at 21 °C. (A) After a 300 s stabilization period, RR(17)PZ (500 nM) was added to the EGFP(Δ 17)hM1 cell suspension (1 mL; 2.5×10^6 cells/mL) and the fluorescence was recorded at 510 nm with time (trace a). Once equilibrium was reached, 5 μ M atropine was added (time 0) in order to initiate the dissociation process (\circ ; 1 every 100 recorded points is shown; trace c). The monoexponential fit for dissociation is shown (solid line). In a control experiment (\blacklozenge), 5 μ M atropine was added prior to RR(17)PZ (500 nM) and recordings (trace b) proceeded for the whole duration of the experiment (1 every 50 recorded points is shown). Inset: The association trace is normalized and presented on a logarithmic scale. F0 refers to the maximal FRET amplitude obtained at equilibrium, and F refers to the fluorescent signal remaining at each time point. Monoexponential (dashed line) and two-exponential (solid line) fits for the association trace are shown. (B) Time recordings of fluorescence amplitude of EGFP(Δ 17)hM1 cells at various RR(17)PZ concentrations (5–800 nM). The ligand was added at time 0, and fluorescence was recorded at 510 nm (four points per second). The best-fit for a two-exponential decay of fluorescence superimposed to a constant linear drift (slope -0.002 s^{-1}) is shown for each experimental trace. (C) Occupancy curve for RR(17)PZ binding to EGFP-(Δ 17)hM1 receptors. Amplitudes for maximal fluorescence extinction, either measured at time 2000 s (\blacksquare) or calculated from the two-exponential fitting of experimental traces in Figure 2B, including (\circ) or not (\triangle) a linear drift (slope -0.002 s^{-1}), are plotted as a function of RR(17)PZ concentration. Best fits to the empirical Hill equation derived for saturation are shown. Maximal FRET amplitudes (%), K_d (nM), and nH values are, respectively: \blacksquare (52, 20, and 1.04), \triangle (53, 19, and 0.96), and \circ (48, 23, and 1.2).

taken into account in two-exponential fitting of the traces. Plotting maximal amplitudes of fluorescence extinction vs RR(17)PZ concentration yields (Figure 2C), for the typical experiment shown in Figure 2B, a saturation curve that best fits with a single category of sites (n_H close to 1). Whatever the way of determination and the fitting procedure, K_d values (19–23 nM) and maximal FRET amplitudes (48–52%) are similar. Two-exponential fitting not only resists the introduction of a linear drift but also is essential for a satisfactory description of the binding process of the ligand, over the whole concentration range. Thus, the association process of RR(17)PZ, and that of all of the probes presented in this work, involves a fast and a slow binding component, the latter becoming more prominent as the ligand concentration increases. This is reminiscent of other reports on complex antagonist binding at muscarinic receptors, interpreted in terms of ligand-induced receptor isomerization^{23,24} or ligand translocation according to a tandem two-site model for ligand binding.²⁵ These mechanisms still deserve further investigation.

Binding parameters for the interaction of all ligands with the fluorescent receptor have been determined either from competition ($[^3\text{H}]\text{QNB}$ binding) or from saturation (FRET amplitudes determined at equilibrium and/or by two-exponential fitting of association traces) experiments. The results are listed in Table 2.

The control compound pirenzepine exhibits (as do several other muscarinic ligands¹⁴) an affinity very similar to that determined for wt hM1 receptors expressed in different cell lines,^{18,26} indicating that the receptor chimera with a truncated N terminus has unaltered drug binding properties.¹⁴ Two Bodipy derivatives, lacking the pirenzepine moiety [Bo(5)] or carrying a short isopeptidic type linker [Bo(6)PZ], are very poor competitors. All other compounds carrying the pirenzepine moiety exhibit fairly good affinities. Some of them, Bo(10)PZ and Bo(24)PZ, bind to the receptor even more tightly than does pirenzepine.

A favorable factor contributing to these high affinities probably is the point of attachment of the linkers to the distal piperazinyl nitrogen of pirenzepine, as shown by Karton and co-workers.¹⁸ These authors indeed showed that lengthening the *N*-methyl group of pirenzepine into a series of long chain *n*-alkylamines (up to 10 methylenes) results in a gradual transformation of the potent antagonist into a weak ($n = 2-6$) and then again potent ($6 < n \leq 10$), but less selective, antagonist. In the Bodipy series, the results obtained with Bo(6)PZ (six atoms linker) and Bo(10)PZ (12 atoms linker) are in complete agreement with their findings. We further show that increasing linker length beyond 10 atoms does not significantly improve binding affinity, unless a 24 atom long chain [Bo(24)PZ] is inserted between pirenzepine and Bodipy. Finally, three pirenzepine derivatives carrying different fluorophores at the end of linkers of similar length [Bo(15)PZ, RR(17)PZ, and Cy3(15)PZ] bind to the receptor with comparable affinities.

We observe the tendency of most compounds to exhibit slightly higher affinities when tested under FRET conditions, as compared to radioligand binding studies. This may stem from differences in incubation temperature (21 °C, FRET; 37 °C, QNB), from possible nonequilibrium [$^3\text{H}]\text{QNB}$ competition conditions, or

Table 2. Summary of Binding Characteristics of the Various Fluorescent Ligands at EGFP-Fused hM1 Receptors^a

compound	[³ H]QNB K_i value (nM) (mean \pm SE; n)	FRET K_d value (nM) (mean \pm SE; n)	maximal FRET amplitude (%) (mean \pm SE; n)	FRET efficacy (E) (mean \pm SE)	R (\AA) (mean \pm SE)
pirenzepine	23.5 \pm 0.8 ($n = 2$)	20 \pm 3 ^b			
Bo(5)	> 1000 ($n = 2$)		0 at 1.2 μ M		
Bodipy derivatives of pirenzepine					
Bo(6)PZ	> 1000 ($n = 2$)		0 at 1 μ M		
Bo(10)PZ	8.8 \pm 2.7 ($n = 3$)	12.9 \pm 0.3 ($n = 5$)	45.0 \pm 0.6 ($n = 6$)	0.63 \pm 0.03	45.4 \pm 0.5
Bo(12)PZ	45.4 \pm 2.9 ($n = 4$)	21.9 \pm 1.4 ($n = 4$)	43.0 \pm 0.9 ($n = 4$)	0.60 \pm 0.03	46.3 \pm 0.6
Bo(15)PZ	69.7 \pm 12.4 ($n = 3$)	14.2 \pm 1.7 ($n = 4$)	34.1 \pm 1.2 ($n = 4$)	0.48 \pm 0.03	50.3 \pm 0.8
Bo(22)PZ	55.1 \pm 9.5 ($n = 4$)	12.7 \pm 1.3 ($n = 4$)	36.4 \pm 0.7 ($n = 4$)	0.51 \pm 0.03	49.3 \pm 0.6
Bo(24)PZ	8.9 \pm 1.0 ($n = 4$)	4.1 \pm 0.9 ($n = 4$)	37.9 \pm 0.1 ($n = 4$)	0.53 \pm 0.02	48.5 \pm 0.5
Rhodamine Red-X derivative of pirenzepine					
RR(17)PZ	53.5 \pm 8.7 ($n = 3$)	18.7 \pm 1.6 ($n = 4$)	48.5 \pm 1.6 ($n = 8$)	0.68 \pm 0.03	45.4 \pm 0.8
Cy3 derivative of pirenzepine					
Cy3(15)PZ	135 \pm 35 ($n = 2$)	35.7 \pm 3.2 ($n = 5$)	42.9 \pm 0.8 ($n = 5$)	0.60 \pm 0.03	57.1 \pm 0.9

^a Apparent dissociation constants are from radioligand- or FRET-based binding assays. FRET efficacy and distance R values are calculated from maximal specific FRET amplitudes using R_0 values (determined for each donor-acceptor pair with κ^2 set at 2/3) listed in Table 1. Values are mean values \pm SE for n independent experiments. ^b K_i value taken from FRET competition experiments using Bo(10)PZ.¹⁴

from nonspecific adsorption of the compounds. Indeed, differential adsorption of several fluorescent ligands to radioligand binding test tubes was detected (not shown).

Estimation of Donor-Acceptor Separation. According to Förster's equations,²⁷ donor-acceptor distances (R values) separating EGFP from Bodipy, Rhodamine Red, or Cy3 can be estimated from the Förster radius (R_0 parameter) characteristic of each donor-acceptor pair and from energy transfer efficiencies. R_0 values (Table 1) were calculated assuming dynamic random averaging of donor-acceptor dipole orientations ($K^2 = 2/3$).¹⁵ Maximal amplitudes of energy transfer, recorded at equilibrium and at ligand saturation, are listed in Table 2 together with FRET efficiencies.

Two groups of molecules are detected according to FRET efficiencies, which are close to 0.5 [Bo(15, 22, or 24)PZ] or close to 0.6 [Bo(10, 12)PZ, RR(17)PZ, and Cy3(15)PZ]. Note also the significant improvement in signal sensitivity (maximal FRET amplitude at saturation) and FRET efficiency obtained with RR(17)PZ, as compared to the reference Bo(10)PZ compound.

The calculated donor-acceptor distances (mean R values; Table 2) indicate that all but one fluorophore [Cy3 in Cy3(15)PZ] are separated from EGFP by a distance ranging from 45 to 50 \AA . Within the Bodipy series, subtle distance variations are found, but they do not correlate with linker length variations. For instance, the fluorophore of Bo(10)PZ and Bo(12)PZ is only 3–4 \AA closer to EGFP than that of Bo(15, 22, 24)PZ derivatives, which carry longer linkers extending from 15 to 24 atoms (potentially ranging from 16 to 27 \AA ; Figure 1B). One possibility that could account for such an observation is that the Bodipy group, locked within a receptor pocket, would not adopt a random orientation but would exhibit a preferred orientation relative to the EGFP fluorophore.

We thus considered the possibility that Bodipy adopts a range of static orientations ($K^2 = 0.476$).¹⁵ Using the corresponding R_0 value (46.9 \AA), donor-acceptor separations (\AA) for Bo(15)PZ (47.6), Bo(22)PZ (46.6), and Bo(24)PZ (45.9) become close to those determined for Bo(10)PZ and Bo(12)PZ (calculated with K^2 value set at 2/3). In other words, there could be a binding site for Bodipy on the receptor protein. Bodipy would either

locate near (3–4 \AA) to this secondary site [Bo(10, 12)-PZ] or would bind to it with a probable preferred orientation [Bo(15, 22, 24)PZ], therefore accounting for the absence of direct correlation between linker length and energy transfer efficiency. The increase in length and/or flexibility of the linker may favor optimal binding of Bodipy within this specific binding area carried by the receptor and may contribute, to some extent, to binding affinity improvement (over pirenzepine alone), as seen with the Bo(24)PZ derivative.

The substitution of Bodipy for Rhodamine Red-X [RR(17)PZ] leads to the determination of a distance very comparable to that found for Bo(10)PZ and Bo(12)PZ, with K^2 set at 2/3 for all of them. In contrast, Cy3 appears to be 10 \AA farther from EGFP as compared to the other fluorophores. Thus, this dye either locates in another subsite or exhibits a particular K^2 value with EGFP (a K^2 value of 0.2, with the corresponding R_0 value of 50 \AA , would give a R value of 46.7 \AA), two hypotheses that remain to be evaluated.

Altogether, these results strongly argue in favor of the existence of a binding site that accommodates Bodipy and Rhodamine Red, in addition to the pirenzepine binding domain.²⁸ This secondary receptor site would be large enough to accommodate bulky and hydrophobic dyes without altering the overall nanomolar affinity of the ligand for the receptor. Thus, provided the linker is long enough ($n \geq 10$) and whatever its nature, both the pirenzepine and the fluorophore may bind to adjacent binding pockets on the receptor.

Such a bitopic topology has also been proposed on the basis of pirenzepine¹⁸ and telenzepine¹² amine congener approaches and of extensive structure-activity relationships, chemical labeling, and mutagenesis studies (see, for a review, ref 29).

Ligand Dissociation Kinetics and Their Modulation by Brucine. Ligand binding kinetics can be readily monitored through FRET. As ligand association processes are complicated due to fast and slow binding components, determinations of association rate constants and of kinetically derived K_d values require extensive analyses. Comparison of the binding properties of pirenzepine derivatives at the EGFP(Δ 17)hM1 chimera can nonetheless be carried out through analysis of their dissociation kinetics.

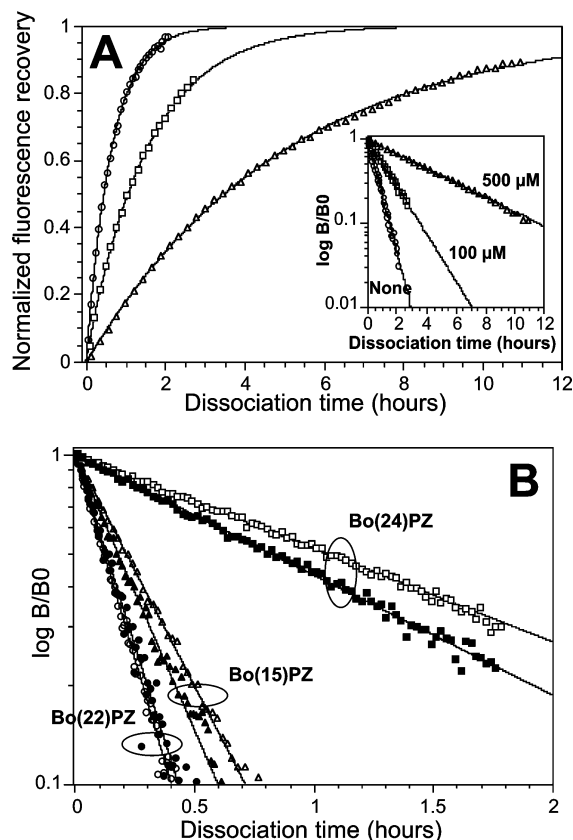


Figure 3. Effect of brucine on the dissociation of Bodipy derivatives from M1 receptors. (A) EGFP($\Delta 17$)hM1 expressing cells were preincubated for 30 min at 21 °C in the presence of 100 nM Bo(10)PZ. Thereafter, atropine (5 μ M) in the absence (○) or the presence of brucine (□, 100 μ M; △, 500 μ M) was added (time 0) and the fluorescence was recorded over time at 510 nm [one point per 2 (○), 4 (□), or 10 (△) s]. Experimental traces (highlighted by the corresponding symbols) are normalized according to total FRET amplitude, i.e., Bo(10)PZ binding at equilibrium (total FRET extinction). Monoexponential fits (hairline) are superimposed to the traces. Inset: Logarithmic representation of the dissociation traces. B represents residual Bo(10)PZ binding (fluorescence signal extinction) at each time point of dissociation, and B_0 represents initial Bo(10)PZ binding at equilibrium (total FRET extinction). A total of 30 time points are shown together with a monoexponential fit to the data. (B) EGFP($\Delta 17$)hM1 expressing cells were preincubated at 21 °C with Bo(15)PZ (200 nM, 20 min, triangles), Bo(22)PZ (200 nM, 20 min, circles), or Bo(24)PZ (100 nM, 30 min, squares). Dissociation started with the addition of 5 μ M atropine alone (open symbols) or combined with 500 μ M brucine (filled symbols). The logarithmic representation of the data and the monoexponential fitting of the traces are as in panel A. k_{off} values (10^{-4} s^{-1}), determined in the absence and the presence of brucine, respectively, are as follows: Bo(15)PZ (9 and 10.7), Bo(22)PZ (15.9 and 14.2), and Bo(24)PZ (1.8 and 2.5).

A 5 μ M saturating concentration of atropine was added to ligand–receptor complexes, at equilibrium, and the EGFP fluorescence emission was recorded with time. For all ligands, dissociation steps (see Figure 3 for an example) can be adjusted using monoexponential fitting of the experimental trace and described by single off-rate constants. As shown in Table 3, large differences in k_{off} values (ranging from 2.6 to 15.7 10^{-4} s^{-1}) are found among ligands.

The alteration of ligand dissociation kinetics by brucine was examined in order to evaluate the impact of the fluorophore nature, of its location, or of its linker

size on discrete receptor–ligand conformations or modulatory processes. Indeed, the hallmark of all prototypical allosteric modulators, including brucine, at muscarinic receptors is their ability to slow ligand (generally [^3H]NMS) dissociation.^{30–32} This is, however, not indicative of magnitude and direction of affinity changes as brucine exhibits various degrees of positive, neutral, or negative binding cooperativity, depending on the orthosteric ligand and the receptor subtype, which is considered.^{16,17,30–33}

Figure 3 presents typical dissociation traces that were obtained for four Bodipy analogues. Once fluorescent ligand binding equilibrium was reached, atropine (5 μ M) was added at time 0 in the absence or presence of brucine (100 or 500 μ M). Figure 3A shows that brucine induces a concentration-dependent retardation of Bo(10)PZ dissociation, indicative of its noncompetitive mode of action. The dissociation process can be described by a single exponential (Figure 3A, inset) with k_{off} values (10^{-4} s^{-1}) progressively decreasing from 4.3 (control) to 1.8 and 0.6 (in the presence of 100 and 500 μ M brucine, respectively). Similarly, brucine slows down Bo(12)PZ dissociation by 6- (100 μ M) and 12 (500 μ M)-fold (Table 3).

In an additional experiment (not shown), brucine (tested over a 3–500 μ M concentration range) was found to halve the k_{off} value for Bo(12)PZ at 10 μ M. This EC_{50} value may be considered as a good estimate of brucine's K_d value for these ligand–receptor complexes.^{30,32} Thus, Bo(10)PZ and Bo(12)PZ binding to the EGFP($\Delta 17$)hM1 chimera is well-modulated by brucine, within a concentration range compatible with the affinity (10–30 μ M) reported for this modulator at [^3H]NMS-occupied M1 receptors.^{17,33}

Finally, we observed that a series of other classical allosteric ligands such as gallamine, alcuronium, and W84, sharing the same conventional mode of allosteric action,³⁴ are also able (at 100 μ M) to decrease the Bo(10)PZ dissociation rate, however, less efficiently than brucine (not shown).

Surprisingly, brucine, even at 500 μ M, is unable to slow Bo(15, 22, 24)PZ dissociation kinetics (Figure 3B). Off-rate constants (mean values determined from a number of independent experiments) do not vary significantly whether brucine is present or not (Table 3). The same is observed for RR(17)PZ while a weak retardation effect can be detected for Cy3(15)PZ.

This is, to our knowledge, the first description of muscarinic ligands that bind in an atropine sensitive manner to M1 receptors and whose dissociation process escapes from brucine modulation, even at high concentrations. Brucine “insensitivity” of ligand dissociation is clearly associated with the presence of a long linker (15 atoms or more) connecting pirenzepine to the fluorophore moiety, whatever its nature. Within the homogeneous Bodipy series, brucine effectiveness sharply depends on linker size. Noteworthy, the brucine sensitive and insensitive ligands belong to the two groups of Bodipy derivatives that were previously defined on the basis of donor–acceptor separation (Table 2).

Thus, the hypothesis, reconciling all observations, could be that the fluorophore entity might have access to a receptor area, distinct from the orthosteric ligand binding site, which could be the allosteric binding pocket to which brucine binds. This would account for the

Table 3. Dissociation Rate Constants for the Interaction of the Various Fluorescent Derivatives with EGFP(Δ 17)hM1 Receptors and Their Alteration by Brucine^a

compound (nM)	dissociation rate constants (s ⁻¹ ; mean values $\times 10^{-4} \pm$ SE)		
	control	+ brucine (100 μ M)	+ brucine (500 μ M)
Bodipy derivatives			
Bo(10)PZ (100)	5.5 \pm 0.8 (<i>n</i> = 4)	2.0 \pm 0.1 (<i>n</i> = 3)	0.72 \pm 0.06 (<i>n</i> = 4)
Bo(12)PZ (200)	15.7 \pm 0.4 (<i>n</i> = 6)	2.5 \pm 0.2 (<i>n</i> = 5)	1.3 \pm 0.2 (<i>n</i> = 3)
Bo(15)PZ (200)	10.3 \pm 0.9 (<i>n</i> = 3)	9.9 \pm 0.3 (<i>n</i> = 2)	11.3 \pm 0.6 (<i>n</i> = 2)
Bo(22)PZ (200)	15.0 \pm 0.3 (<i>n</i> = 4)	14.4 \pm 0.3 (<i>n</i> = 2)	14.6 \pm 0.4 (<i>n</i> = 2)
Bo(24)PZ (100)	2.6 \pm 0.4 (<i>n</i> = 4)	2.3 \pm 0.2 (<i>n</i> = 3)	2.5 (<i>n</i> = 1)
Rhodamine Red-X derivative			
RR(17)PZ (500)	6.0 \pm 0.3 (<i>n</i> = 4)	6.2 \pm 0.2 (<i>n</i> = 2)	5.1 \pm 0.5 (<i>n</i> = 3)
Cy3 derivative			
Cy3(15)PZ (300)	5.0 \pm 0.2 (<i>n</i> = 4)	3.9 (<i>n</i> = 1)	3.53 \pm 0.02 (<i>n</i> = 2)

^a Atropine (5 μ M) alone (control) or a mixture of atropine (5 μ M) and brucine (100 or 500 μ M) was added to an EGFP(Δ 17)hM1 cell suspension previously incubated until equilibrium with each ligand at the indicated concentration (given under parentheses). Dissociation was followed at 21 °C as illustrated in Figure 3A. Mean K_{off} values for *n* independent experiments are indicated together with associated SEs.

absence of the brucine effect on Bo(15, 22, 24)PZ, RR(17)PZ, or Cy3(15)PZ dissociation.

Further arguments in favor of this interpretation should come from the analysis of direct competition between these fluorescent pirenzepine derivatives and brucine for binding to its modulatory site. As well, it would be interesting to test whether another series of modulators such as staurosporine, KT5720, PG987, or WIN analogues, which are proposed to bind to a second muscarinic receptor allosteric site,^{35–37} mainly on the basis of their noncompetitive mode of inhibition of the effects of prototypical modulators, are able or not to affect dissociation kinetics of the ligands described here.

Future experiments carried out under equilibrium and kinetic conditions, through FRET and radioligand binding studies, should clarify the molecular mechanisms underlying brucine insensitivity of the various ligands reported here. Point mutagenesis of the receptor combined with molecular modeling should also provide information on the location of the fluorophore binding site(s) and of its (their) possible overlap(s) with the allosteric binding domain(s) borne by the muscarinic M1 receptor.

Conclusion. Donor–acceptor distance measurements and analyses of dissociation kinetics performed in the presence of the allosteric modulator brucine suggest that Bo(15, 22, 24)PZ, RR(17)PZ, or Cy3(15)PZ may behave as new and atypical ligands for the muscarinic M1 receptor. They may simultaneously occupy both the orthosteric (through the pirenzepine group) and an allosteric (through the fluorophore moiety) site on the receptor protein.

Such a bitopic character opens unusual pharmacological perspectives in terms of intrinsic modulatory properties. For example, anchoring a bulky group (mimicking the fluorophore here), through a linker, to an agonistic ligand structure could modulate its subtype selectivity and possibly potency and efficacy.

Although the present study tends to indicate that this is probably a difficult challenge, fluorescent agonists or allosteric modulators, taken as distinct molecular species, represent ideal (although missing) tools that would allow us to monitor, in real-time, on living cells and in parallel to physiological responses, ligand binding to— as well as functionality and regulation of—different conformational states of muscarinic receptors.^{7,38,39}

Experimental Section

General Methods. All chemicals were obtained from commercial suppliers and used without further purification. Succinimidyl esters of Bodipy [558/568] and Rhodamine Red-X [560/580] as well as Bodipy [558/568]pirenzepine dihydrochloride were purchased from Molecular Probes. Fluorolink Cy3 [550/570] succinimidyl ester was from Amersham Pharmacia Biotech.

Pyridine was dried over KOH, and DMF was dried on P₂O₅ and distilled from KOH at 70 °C under reduced pressure. Tetrahydrofuran (THF) was distilled from sodium-benzophenone. Methylene chloride (CH₂Cl₂) was distilled from CaH₂.

All ¹H and ¹³C NMR spectra were recorded on a Bruker DPX spectrometer at 200 or 300 MHz for the ¹H NMR spectra and at 50 or 75 MHz for the ¹³C NMR spectra. NMR chemical shifts are expressed in ppm relative to internal solvent peaks, and coupling constants (*J*) are measured in Hertz. The signals are described as s (singlet), d (doublet), t (triplet), m (multiplet), and br s (broad singlet). Electrospray ionization (ESI)-MS were recorded on a Perkin-Elmer Biospec mass spectrometer. MALDI-TOF measurements were carried out on a Bruker BIFLEX spectrometer equipped with the SCOUT high-resolution optics. Silica gel 60 (63–200 μ m; Merck) was used for column chromatography. The melting points are measured in open capillary tubes using a Gallekamp apparatus and are uncorrected.

Bo(10)PZ (1). This compound was purchased from Molecular Probes.

N-(2-Chloro-pyridin-3-yl)-2-nitrobenzamide (3). A mixture of 2-nitrobenzoic acid (5 g, 30.0 mmol) and oxalyl chloride (3.67 mL, 42.0 mmol) in THF (140 mL) containing DMF (0.34 mL) was refluxed until a pale yellow solution was obtained (1 h). The excess oxalyl chloride was removed under reduced pressure, and the residue was then dissolved in THF. Pyridine (14.5 mL, 180 mmol) and 3-amino-2-chloropyridine (3.85 g, 30 mmol) were added. After 2 h at room temperature, the mixture was diluted with CH₂Cl₂ (200 mL), washed with 1 N HCl, 10% NaHCO₃, and brine solutions (150 mL each), and dried over MgSO₄. The solvent was removed under reduced pressure, and the product was recrystallized from CHCl₃ (5.55 g, 67%); mp 152 °C (lit. 152 °C).⁴⁰ ¹H NMR [(CD₃)₂SO, 200 MHz]: δ 10.6 (br s, 1 H), 8.29–8.32 (dd, *J*₁ = 4.6 Hz, *J*₂ = 1.2 Hz, 1 H), 8.17–8.22 (m, 2 H), 7.74–7.94 (m, 3 H), 7.50–7.57 (dd, *J*₁ = 8.0 Hz, *J*₂ = 5.0 Hz, 1 H). ¹³C NMR [(CD₃)₂SO, 50 MHz]: δ 165.1, 146.4, 135.2, 134.2, 131.2, 129.2, 124.3, 123.5.

2-Amino-N-(2-chloropyridin-3-yl)benzamide (4). To a solution of **3** (5 g, 18.0 mmol) in 36% HCl (20 mL), stannous chloride (17.1 g, 90.1 mmol) solubilized in concentrated HCl (10 mL) at 50–60 °C was added. The mixture was heated to 100 °C for 15 min, cooled, and filtered to give a white crystalline solid, which was dissolved in water. The aqueous solution was basified with 1 N NaOH and extracted three times with CHCl₃. The organic layers were combined, dried

over MgSO_4 , filtered, and evaporated to give **4** (3.86 g, 86%); mp 175 °C (lit. 175 °C).⁴⁰ ^1H NMR [$(\text{CD}_3)_2\text{SO}$, 200 MHz]: δ 9.90 (br s, 1 H), 8.27–8.30 (dd, $J_1 = 4.6$ Hz, $J_2 = 1.7$ Hz, 1 H), 8.04–8.09 (dd, $J_1 = 7.8$ Hz, $J_2 = 1.7$ Hz, 1 H), 7.71–7.76 (dd, $J_1 = 8.0$ Hz, $J_2 = 1.2$ Hz, 1 H), 7.45–7.53 (dd, $J_1 = 7.8$ Hz, $J_2 = 1.46$ Hz, 1 H), 7.20–7.28 (td, $J_1 = 8.3$ Hz, $J_2 = 1.2$ Hz, 1 H), 6.78 (d, $J = 8.3$ Hz, 1 H), 6.57–6.67 (td, $J_1 = 7.8$ Hz, $J_2 = 1.0$ Hz, 1 H), 6.48 (br s, 1 H). ^{13}C NMR [$(\text{CD}_3)_2\text{SO}$, 50 MHz]: δ 167.8, 150.3, 146.3, 136.5, 132.7, 132.4, 128.8, 123.4, 116.7, 114.9, 113.4.

5,11-Dihydro-6H-pyrido[2,3-b]-1,4-benzodiazepin-6-one (5). Product **4** (3 g, 12.1 mmol) was heated for 5 min in a metallic bath at 210 °C. The cyclization with formation of HCl took place at 205 °C. After the mixture was cooled, the solid product was dissolved in boiling ethanol. Cooling overnight at 0 °C gave **5** (2.04 g, 80%); mp 283 °C (lit. 286–289 °C).²⁰ ^1H NMR [$(\text{CD}_3)_2\text{SO}$, 300 MHz]: δ 9.97 (br s, 1 H), 8.77 (br s, 1 H), 7.89–7.91 (dd, $J_1 = 4.0$ Hz, $J_2 = 1.0$ Hz, 1 H), 7.71–7.74 (dd, $J_1 = 8.1$ Hz, $J_2 = 1.5$ Hz, 1 H), 7.34–7.40 (m, 2 H), 7.12 (d, $J = 8.1$ Hz, 1 H), 6.90–7.00 (m, 2 H). ^{13}C NMR [$(\text{CD}_3)_2\text{SO}$, 50 MHz]: δ 167.0, 150.5, 146.7, 141.3, 133.7, 132.2, 129.2, 124.8, 121.7, 121.3, 119.6, 118.6.

11-(Chloroacetyl)-5,11-dihydro-6H-pyrido[2,3-b]-[1,4]benzodiazepin-6-one (6). A suspension of **5** (500 mg, 2.37 mmol) in dioxane (10 mL) was refluxed for 15 min and then allowed to cool to room temperature before adding Et_3N (0.4 mL, 2.85 mmol). Chloroacetyl chloride (0.23 mL, 2.85 mmol) was added dropwise, under stirring, to this solution during a period of 30 min. The mixture was then refluxed for 8 h. After the mixture was cooled, the precipitate was removed by filtration on a Celite pad and washed with dioxane. The crude filtrate was evaporated and purified by silica gel column chromatography (EtOAc/heptane 3/7 to 7/3) to give **6** (480 mg, 70%); mp 212 °C (lit. 212–219 °C). ^1H NMR [$(\text{CD}_3)_2\text{SO}$, 200 MHz]: δ 10.86 (br s, 1 H), 8.28–8.32 (dd, $J_1 = 4.6$ Hz, $J_2 = 1.7$ Hz, 1 H), 7.80–7.83 (dd, $J_1 = 8.3$ Hz, $J_2 = 1.7$ Hz, 1 H), 7.65–7.73 (td, $J_1 = 7.8$ Hz, $J_2 = 1.5$ Hz, 2 H), 7.42–7.59 (m, 3 H), 4.36 (br s, 2 H). ^{13}C NMR [$(\text{CD}_3)_2\text{SO}$, 50 MHz]: δ 165.9, 144.7, 133.2, 131.1, 128.6, 127.8, 125.1, 42.2.

N-Boc Piperazine (8). A solution of piperazine (3 g, 34.9 mmol) in CH_2Cl_2 (50 mL) was cooled at 0 °C. Di-*tert*-butyl dicarbonate (1.52 g, 6.98 mmol) dissolved in CH_2Cl_2 (25 mL) was added dropwise. The resulting mixture was stirred at room temperature overnight, filtered, and concentrated under reduced pressure. The crude product was dissolved in brine (50 mL) and extracted with ether (3 \times 50 mL). The organic layer was dried over MgSO_4 , filtered, evaporated, and purified by silica gel column chromatography (EtOAc/MeOH 9/1) to give **8** (974 mg, 75%); mp 70 °C. ^1H NMR (CDCl_3 , 300 MHz): δ 3.29 (t, $J = 5.1$ Hz, 4 H), 2.71 (t, $J = 5.0$ Hz, 4 H), 1.56 (br s, 1 H), 1.38 (s, 9 H). ^{13}C NMR (CDCl_3 , 75 MHz): δ 162.2, 79.3, 45.8, 45.0, 28.3. MS (ESI-TOF, 80 eV) m/z 186.14 ($\text{C}_9\text{H}_{18}\text{N}_2\text{O}_2$), 187.11 ($\text{M} + \text{H}$)⁺.

4-[4-(1,3-Dioxo-1,3-dihydro-isoindol-2-yl)butyl]piperazine-1-carboxylic Acid *tert*-Butyl Ester (10). *N*-(4-Bromobutyl)phthalimide (378.7 mg, 1 equiv) and DIPEA (0.23 mL, 1 equiv) were added to a solution of *tert*-butyl 1-piperazine carboxylate (250 mg), in anhydrous CH_3CN . The mixture was refluxed under argon for 12 h. After it was evaporated to dryness, the crude product was washed with a saturated solution of Na_2CO_3 and extracted with EtOAc. The organic layer was dried over Na_2SO_4 , filtered, and evaporated. The expected compound was purified by silica gel column chromatography (EtOAc/heptane 1/1), giving a white solid (95%); mp 45 °C. ^1H NMR (CDCl_3 , 300 MHz): δ 7.82 (m, 2 H), 7.72 (m, 2 H), 3.71 (m, 2 H), 3.41 (m, 4 H), 2.36 (m, 6 H), 1.69 (m, 2 H), 1.53 (m, 2 H), 1.45 (s, 9 H). MS (ESI-TOF, 80 eV) m/z 387.22 ($\text{C}_{21}\text{H}_{29}\text{N}_3\text{O}_4$), 388.20 ($\text{M} + \text{H}$)⁺.

4-(4-Amino-butyl)piperazine-1-carboxylic Acid *tert*-Butyl Ester (11). Hydrazine monohydrate (0.1 mL, 2.06 mmol) was added to a solution of the phthalimide **10** (400 mg, 1.03 mmol) dissolved in a minimal volume of ethanol. The mixture was refluxed for 8 h. The white precipitate was filtered off, and the filtrate was evaporated. The compound was

dissolved in EtOAc and washed with a saturated solution of Na_2CO_3 , water, and brine. The organic layer was dried over Na_2SO_4 , filtered, and evaporated to dryness, giving the expected compound **11** in a quantitative yield. ^1H NMR (CDCl_3 , 200 MHz): δ 3.36 (m, 4 H), 2.69 (m, 2 H), 2.29–2.38 (m, 6 H), 1.87 (s, 2 H), 1.44 (m, 13 H). ^{13}C NMR (CDCl_3 , 50 MHz): δ 154.9, 79.7, 58.5, 53.1, 43.7, 41.8, 31.1, 28.5, 24.2.

6-(1,3-Dioxo-1,3-dihydro-isoindol-2-yl)hexanoic Acid (13). Na_2CO_3 (425 mg, 4.19 mmol) was added to a solution of 6-amino-hexanoic acid (1 g, 4.57 mmol) dissolved in water (10 mL). *N*-Carbathoxyphthalimide (500 mg, 3.8 mmol) was added to the solution, and the mixture was stirred at room temperature for 1 h. Acidification to pH 2–3 was done with 1 N HCl. The formed precipitate was filtered off. The filtrate was evaporated to dryness, and compound **13** was obtained after trituration in Et_2O (700 mg, 70%); mp 105 °C. ^1H NMR [$(\text{CD}_3)_2\text{SO}$, 300 MHz]: δ 7.84 (m, 2 H), 7.71 (m, 2 H), 3.69 (t, 2 H, $J = 7.2$ Hz), 2.36 (t, 2 H, $J = 7.5$ Hz), 1.70 (m, 4 H), 1.42 (m, 2 H). MS (ESI-TOF, 80 eV) m/z 261.10 ($\text{C}_{14}\text{H}_{15}\text{NO}_4$), 262.10 ($\text{M} + \text{H}$)⁺.

4-[4-[6-(1,3-Dioxo-1,3-dihydro-isoindol-2-yl)hexanoylamino]butyl]piperazine-1-carboxylic Acid *tert*-Butyl Ester (14). To a solution of compound **11** (356 mg, 1.38 mmol) in anhydrous THF (5 mL), compound **13** (362 mg, 1.38 mmol), HOBt (187 mg, 1.38 mmol), and *N*-methylmorpholine (0.15 mL, 1.38 mmol) were added and the mixture was stirred at room temperature for 10 min. The mixture was then cooled to 0 °C, and DCC (314 mg, 1.52 mmol) in 2 mL of THF was added dropwise. Stirring was pursued at room temperature during 10 h. The precipitate was filtered off and washed with THF, and the filtrate was evaporated. The mixture was then washed with 10% Na_2CO_3 and extracted with EtOAc. The organic layer was dried over Na_2SO_4 , filtered, and evaporated. Compound **14** was isolated as a white solid after trituration in ether (624 mg, 90%). ^1H NMR [$(\text{CD}_3)_2\text{SO}$, 300 MHz]: δ 7.83 (m, 4 H), 5.57 (s, 1 H), 3.54 (t, 2 H, $J = 6.9$ Hz), 3.27 (m, 4 H), 2.98 (m, 2 H), 2.24 (m, 4 H), 2.01 (t, 2 H, $J = 7.5$ Hz), 1.01–1.68 (m, 21 H). ^{13}C NMR [$(\text{CD}_3)_2\text{SO}$, 75 MHz]: δ 172.3, 168.5, 154.4, 134.9, 132.2, 123.6, 79.2, 58.0, 53.1, 40.1, 38.8, 37.9, 35.8, 34.0, 28.6, 28.4, 27.6, 26.5, 24.2. MS (ESI-TOF, 80 eV) m/z 500.30 ($\text{C}_{27}\text{H}_{40}\text{N}_4\text{O}_5$), 501.27 ($\text{M} + \text{H}$)⁺, 523.26 ($\text{M} + \text{Na}$)⁺.

6-(1,3-Dioxo-1,3-dihydro-isoindol-2-yl)hexanoic Acid (4-Piperazin-1-yl-butyl)amide, HCl Salt (15). Deprotection of the Boc protecting group of compound **14** (100 mg, 0.20 mmol) dissolved in EtOAc was achieved by using HCl gaz (flux maintained for 2 min). The mixture was then stirred for 1 h at room temperature, and the product **15** was recovered as a hydrochloride salt after triturating in ether (quantitative yield). ^1H NMR [$(\text{CD}_3)_2\text{SO}$, 200 MHz]: δ 10.06 (s, 1 H), 7.83 (m, 4 H), 4.71 (s, 1 H), 3.34–3.67 (m, 6 H), 2.95 (m, 4 H), 2.78 (t, 2 H, $J = 7.5$ Hz), 2.05 (t, 2 H, $J = 7.2$ Hz), 1.15–1.65 (m, 12 H). MS (ESI-TOF, 80 eV) m/z 400.25 ($\text{C}_{22}\text{H}_{32}\text{N}_4\text{O}_3$), 401.28 ($\text{M} + \text{H}$)⁺.

4-[4-(6-Amino-hexanoylamino)butyl]piperazine-1-carboxylic Acid *tert*-Butyl Ester (16). Compound **16** was obtained in a quantitative yield using the experimental procedure already described for **11**. ^1H NMR [$(\text{CD}_3)_2\text{SO}$, 300 MHz]: δ 6.53 (s, 2 H), 3.65 (m, 2 H), 3.25 (m, 4 H), 2.95 (m, 2 H), 2.26 (m, 4 H), 2.11 (t, 2 H, $J = 7.6$ Hz), 1.04–1.71 (m, 21 H). MS (ESI-TOF, 80 eV) m/z 370.29 ($\text{C}_{19}\text{H}_{38}\text{N}_4\text{O}_3$), 371.31 ($\text{M} + \text{H}$)⁺.

6-(1,3-Dioxo-1,3-dihydro-isoindol-2-yl)hexanoic Acid [5-(4-Piperazin-1-yl-butylcarbamoyl)pentyl]amide, HCl Salt (17). To a solution of compound **16** (78 mg, 0.21 mmol) in anhydrous THF (1.5 mL), compound **13** (54.9 mg, 0.21 mmol), HOBt (28.4 mg, 0.21 mmol), and *N*-methylmorpholine (0.023 mL, 0.21 mmol) were added and the mixture was stirred for 10 min at room temperature. The solution was then cooled to 0 °C, and a solution of DCC (47.7 mg, 0.23 mmol) in THF was added dropwise. Stirring was pursued for 10 h at room temperature. The formed precipitate was filtered off and washed with THF, and the filtrate was evaporated to dryness. The mixture was dissolved in EtOAc and washed with a solution of 10% Na_2CO_3 , water, and brine. The organic layer

was dried over Na_2SO_4 , filtered, and evaporated. The mixture was submitted to purification on silica gel (EtOAc/heptane 1/1) to give the expected Boc-protected intermediate in 80% yield as a white solid. $^1\text{H NMR}$ [$(\text{CD}_3)_2\text{SO}$, 300 MHz]: δ 7.68–7.83 (m, 4H), 3.54 (t, 2 H, $J = 6.84$ Hz), 3.28 (m, 8 H), 2.96 (m, 4 H), 2.24 (m, 6 H), 2.00 (m, 4 H), 1.07–1.56 (m, 21 H). $^{13}\text{C NMR}$ [$(\text{CD}_3)_2\text{SO}$, 75 MHz]: δ 172.4, 172.3, 168.5, 166.1, 135.0, 132.2, 123.6, 79.3, 58.1, 53.1, 48.1, 40.7, 40.1, 38.8, 37.9, 36.0, 33.9, 29.5, 28.7, 28.4, 27.7, 26.7, 25.7, 25.1, 24.2, 20.9. MS (ESI-TOF, 80 eV) m/z 613.38 ($\text{C}_{33}\text{H}_{51}\text{N}_5\text{O}_6$), 614.41 ($\text{M} + \text{H}$) $^+$, 636.38 ($\text{M} + \text{Na}$) $^+$.

The *N*-Boc protecting group was then removed according to the procedure described for compound **15** giving the hydrochloride **17** in a quantitative yield. $^1\text{H NMR}$ [$(\text{CD}_3)_2\text{SO}$, 300 MHz]: δ 9.64 (br s, 1 H), 7.70–7.84 (m, 4 H), 3.58 (m, 2 H), 3.27–3.31 (m, 8 H), 2.95–3.01 (m, 4 H), 2.22–2.24 (m, 6 H), 2.01–2.06 (m, 4 H), 1.10–1.63 (m, 14 H). $^{13}\text{C NMR}$ [$(\text{CD}_3)_2\text{SO}$, 75 MHz]: δ 172.5, 172.2, 168.3, 134.8, 132.0, 123.4, 55.7, 48.1, 40.3, 38.9, 38.2, 37.9, 35.9, 35.7, 29.5, 28.3, 26.8, 26.7, 26.5, 25.6, 25.5. MS (ESI-TOF, 135 eV) m/z 513.33 ($\text{C}_{28}\text{H}_{43}\text{N}_5\text{O}_4$), 514.36 ($\text{M} + \text{H}$) $^+$.

Ethyl 1,2-Dimethane Sulfonate (19). MsCl (2.43 mL, 31.5 mmol) was added to a solution of EG (930 mg, 15 mmol) in CH_2Cl_2 (75 mL) and Et_3N (4.38 mL, 31.5 mmol) at 0 °C. The mixture was stirred for 1 h at 0 °C followed by 2 h at room temperature. The precipitate was filtered off, and the filtrate was evaporated and purified by chromatography on a silica gel column (heptane/EtOAc 3/7) to give a colorless oil (3.15 g, 96%). $^1\text{H NMR}$ (CDCl_3 , 200 MHz): δ 4.40 (s, 4 H), 3.02 (s, 6 H). $^{13}\text{C NMR}$ (CDCl_3 , 50 MHz): δ 67.0, 35.3. MS (ESI-TOF, 135 eV) m/z 240.98 ($\text{C}_4\text{H}_{10}\text{NaO}_6\text{S}_2$), 240.97 ($\text{M} + \text{Na}$) $^+$.

2-Azidoethyl Methane Sulfonate (20). To a solution of **19** (3.15 g, 14.45 mmol) in dry CH_3CN (75 mL) was added NaN_3 (891 mg, 13.7 mmol), and the mixture was refluxed for 12 h. The precipitate was filtered off, and the filtrate was evaporated and purified by chromatography on a silica gel column with EtOAc/heptane (3/7 to 4/6) to give a colorless oil (1.1 g, 46%). TLC (EtOAc/heptane 4/6) R_f 0.36. $^1\text{H NMR}$ (CDCl_3 , 200 MHz): δ 4.28 (t, $J = 4.4$ Hz, 2 H), 3.69 (t, $J = 4.4$ Hz, 2 H), 3.61 (t, $J = 4.9$ Hz, 2 H), 2.98 (s, 3 H). $^{13}\text{C NMR}$ (CDCl_3 , 50 MHz): δ 67.7, 49.6, 37.4.

***N*-(2-Azidoethyl)piperazine (21)**. To a solution of **20** (817 mg, 4.95 mmol) in dry CH_3CN (20 mL) and Et_3N (1.38 mL, 9.9 mmol) *N*-Boc piperazine **8** (1.1 g, 5.94 mmol) was added. The mixture was refluxed for 16 h, evaporated in vacuo, and chromatographed on a silica gel column (EtOAc to EtOAc/MeOH 9/1) to give a white solid (1.2 g, 95%). $^1\text{H NMR}$ (CDCl_3 , 200 MHz): δ 3.36 (t, $J = 5.1$ Hz, 4 H), 3.25 (t, $J = 6.0$ Hz, 2 H), 2.51 (t, $J = 6.0$ Hz, 2 H), 2.35 (t, $J = 5$ Hz, 4 H), 1.36 (s, 9 H). $^{13}\text{C NMR}$ (CDCl_3 , 50 MHz): δ 154.4, 79.3, 57.0, 52.7, 47.8, 43.2, 28.2.

The formed compound was then subjected to *N*-Boc removal by action of TFA 50% in CH_2Cl_2 . The mixture was evaporated to remove excess TFA. The expected compound was purified by silica gel flash column chromatography (EtOAc/MeOH/ Et_3N 89/10/1) to give **21**. Yield: 70%. $^1\text{H NMR}$ (CDCl_3 , 200 MHz): δ 5.60 (br s, 1 H), 3.32 (t, $J = 5.2$ Hz, 4 H), 3.22 (t, $J = 5.9$ Hz, 2 H), 2.54 (t, $J = 6.0$ Hz, 2 H), 2.42 (t, $J = 5.4$ Hz, 4 H). $^{13}\text{C NMR}$ (CDCl_3 , 50 MHz): δ 57.4, 52.9, 48.0, 44.2.

2-{2-[2-(Triphenylmethoxy)ethoxy]ethoxy}ethyl-methylsulfonate (23). Ph_3COH (3.90 g, 15.0 mmol) was added to a solution of TsOH (0.19 g, 1.0 mmol) in TEG (20 mL, 150 mmol) and benzene (100.0 mL) at room temperature. After the solution was refluxed for 2 h, the solvent was evaporated. The residue was taken up in EtOAc (100 mL), washed with brine (3 \times 50 mL), dried over MgSO_4 , and evaporated in vacuo. The crude product was taken up in CH_2Cl_2 (20.0 mL) and Et_3N (2.36 mL, 17.0 mmol). To this solution was added MsCl (1.27 mL, 16.5 mmol) at 0 °C. After this solution was stirred for 2 h, the solution was allowed to warm to room temperature and stirring was pursued overnight. The precipitate was filtered, the filtrate was evaporated, and the crude product was purified by chromatography on a silica gel column (EtOAc/heptane 5/5) to yield **23** as a white solid (5.84 g, 82%); mp 93 °C. TLC

(EtOAc/heptane 5/5) R_f 0.39. $^1\text{H NMR}$ (CDCl_3 , 200 MHz): δ 7.27–7.37 (m, 15 H), 4.38–4.42 (m, 2 H), 3.82–3.85 (m, 2 H), 3.74 (s, 4 H), 3.70 (t, $J = 5.8$ Hz, 2 H), 3.29 (t, $J = 5.1$ Hz, 2 H), 2.99 (s, 3 H). $^{13}\text{C NMR}$ (CDCl_3 , 50 MHz): δ 144.0, 128.7, 127.7, 126.9, 86.6, 70.7, 69.2, 69.0, 63.3, 37.6. MS (ESI-TOF, 80 eV) m/z 470.17 ($\text{C}_{26}\text{H}_{30}\text{O}_6\text{S}$), 493.18 ($\text{M} + \text{Na}$) $^+$.

[[2-[2-(2-Azidoethoxy)ethoxy]ethoxy](diphenyl)methyl]-benzene (24). Compound **23** (1 g, 2.12 mmol) was refluxed with NaN_3 (207 mg, 3.2 mmol) in dry CH_3CN (30 mL) for 36 h. H_2O (50 mL) was added, and the mixture was extracted with CH_2Cl_2 . After the mixture was dried (MgSO_4) and evaporated, the residue was purified by silica gel column chromatography (EtOAc/heptane 2/8) to give **24** as a colorless liquid (2.24 mg, 84%). TLC (EtOAc/heptane 3/7) R_f 0.25. $^1\text{H NMR}$ (CDCl_3 , 200 MHz): δ 7.22–7.29 (m, 15 H), 3.69–3.72 (m, 8 H), 3.38 (t, $J = 5.0$ Hz, 2 H), 3.30 (t, $J = 5.0$ Hz, 2 H). $^{13}\text{C NMR}$ (CDCl_3 , 50 MHz): δ 144.1, 128.6, 127.6, 126.8, 86.4, 70.7, 69.9, 63.2, 50.6. MS (ESITOF, 80 eV) m/z 417.20 ($\text{C}_{25}\text{H}_{27}\text{N}_3\text{O}_3$), 440.20 ($\text{M} + \text{Na}$) $^+$.

2-[2-(2-Azidoethoxy)ethoxy]ethyl-methylsulfonate (25). To a MeOH solution (35 mL) of **24** (1.2 g, 2.88 mmol) was added TsOH (18 mg, 0.3 mmol), and the resulting mixture was refluxed for 4 h. Na_2CO_3 (610 mg, 5.76 mmol) was added, and the solution was stirred for 5 min before evaporation of the solvent under reduced pressure. CH_2Cl_2 was added to the crude product, and the formed precipitate was filtered. Without further purifications, Et_3N (0.8 mL, 5.76 mmol) and MsCl (0.445 mL, 5.76 mmol) were added at 0 °C. After 2 h, the solution was allowed to warm to room temperature and stirred overnight. The precipitate was filtered off, and the filtrate was evaporated under reduced pressure. The crude product was purified by silica gel column chromatography (EtOAc/heptane 5/5) to give **25** as a colorless oil (524 mg, 72%). TLC (EtOAc/heptane 5/5): R_f 0.21. $^1\text{H NMR}$ (CDCl_3 , 200 MHz): δ 4.27 (t, $J = 4.5$ Hz, 2 H), 3.69 (t, $J = 4.5$ Hz, 2 H), 3.56–3.62 (m, 6 H), 3.29 (t, $J = 4.6$ Hz, 2 H), 2.98 (s, 3 H). $^{13}\text{C NMR}$ (CDCl_3 , 50 MHz): δ 85.7, 70.2, 69.7, 69.1, 68.7, 50.3, 37.2. MS (ESI-TOF, 80 eV) m/z 253.07 ($\text{C}_7\text{H}_{15}\text{N}_3\text{O}_5\text{S}$), 276.06 ($\text{M} + \text{Na}$) $^+$.

1-{2-[2-(2-Azidoethoxy)ethoxy]ethyl}piperazine, TFA Salt (26). To a solution of **25** (710 mg, 2.81 mmol) in dry MeCN (25 mL), Boc piperazine (626 mg, 3.36 mmol) and Et_3N (0.784 mL, 5.62 mmol) were added, and the resulting mixture was refluxed for 20 h. The precipitate was filtered off, and the filtrate was evaporated under reduced pressure. The residue was then chromatographed on a silica gel column (EtOAc/MeOH 95/5). The product was next submitted to 50% TFA in CH_2Cl_2 (5 mL) treatment for 2 h. After evaporation and purification by silica gel column chromatography (EtOAc/MeOH 9/1), compound **26** was obtained as a white solid (380 mg, 56%). TLC (EtOAc/MeOH 85/15) R_f 0.15. $^1\text{H NMR}$ (CDCl_3 , 300 MHz): δ 3.52–3.60 (m, 8 H), 3.30 (t, $J = 5.0$ Hz, 2 H), 3.03 (t, $J = 5.0$ Hz, 2 H), 2.53–2.61 (m, 8 H). $^{13}\text{C NMR}$ (CDCl_3 , 75 MHz): δ 70.5, 70.2, 69.9, 68.7, 57.5, 51.4, 50.5, 44.1. MS (ESI-TOF, 80 eV) m/z 243.17 ($\text{C}_{10}\text{H}_{21}\text{N}_4\text{O}_2$), 244.18 ($\text{M} + \text{H}$) $^+$.

1,1,1-Triphenyl-2,5,8,11,14,17-hexaoxonadecan-19-ol (27). A solution of TEG (6.93 mL, 52 mmol) and *t*-BuOK (4.85 g, 43.25 mmol) in dry *t*-BuOH (150 mL) was refluxed for 30 min. Product **23** (8.16 g, 17.3 mmol) was then added, and the mixture was refluxed for 3 h. The mixture was then, respectively, cooled, washed with brine, extracted with CH_2Cl_2 , dried over MgSO_4 , filtered, and evaporated. The product was purified by silica gel column chromatography (EtOAc/heptane 8/2) to give **27** as a colorless oil (7.47 g, 82%). TLC (EtOAc/heptane 8/2) R_f 0.16. $^1\text{H NMR}$ (CDCl_3 , 200 MHz): δ 7.21–7.32 (m, 15 H), 3.56–3.68 (m, 22 H), 3.25 (t, $J = 5.0$ Hz, 2 H), 2.77 (br s, 1 H). $^{13}\text{C NMR}$ (CDCl_3 , 50 MHz): δ 144.6, 128.6, 127.6, 126.7, 86.4, 72.4, 70.5, 70.2, 62.2, 61.5. MS (ESI-TOF, 135 eV) m/z 524.65 ($\text{C}_{31}\text{H}_{40}\text{O}_7$), 547.23 ($\text{M} + \text{Na}$) $^+$, 563.24 ($\text{M} + \text{K}$) $^+$, 243.09 (PPh_3C) $^+$.

19,19,19-Triphenyl-3,6,9,12,15,18-hexaoxonadec-1-yl-methane Sulfonate (28). Et_3N (2.45 mL, 17.6 mmol) and MsCl (1.36 mL, 17.6 mmol) were added to a solution of **7** (6.14 g, 11.72 mmol) in CH_2Cl_2 (100 mL) at 0 °C. The mixture was stirred for 2 h at 0 °C and overnight at room temperature.

The precipitate was filtered, the filtrate was evaporated, and the desired product was purified by silica gel column chromatography (EtOAc/heptane 7/3) as a colorless oil (6.84 g, 97%). TLC (EtOAc/heptane 7/3) R_f 0.33. ^1H NMR (CDCl_3 , 300 MHz): δ 7.24–7.47 (m, 15 H), 4.37 (t, $J = 4.3$ Hz, 2 H), 3.67–3.77 (m, 18 H), 3.28 (t, $J = 5.1$ Hz, 2 H), 3.06 (s, 3 H). ^{13}C NMR (CDCl_3 , 75 MHz): δ 143.9, 128.5, 127.5, 126.7, 86.2, 70.5, 70.4, 70.3, 70.2, 69.1, 68.7, 63.1, 37.3. MS (ESI-TOF, 80 eV) m/z 602.25 ($\text{C}_{32}\text{H}_{42}\text{O}_9\text{S}$), 625.20 (M + Na), 361.13 (M + H – PPh_3C) $^+$, 243.09 (PPh_3C) $^+$.

1,1,1-Triphenyl-2,5,8,11,14,17,20-heptaaxadocosan-22-ol (29). A solution of EG (0.69 mL, 12.46 mmol) and *t*-BuOK (1.4 g, 12.46 mmol) in dry *t*-BuOH (50 mL) was refluxed for 30 min. Product **28** (2 g, 4.15 mmol) was then added, and the mixture was refluxed for 4 h. The mixture was then cooled, washed with brine, extracted with CH_2Cl_2 , dried over MgSO_4 , filtered, and evaporated. The crude product was then purified by silica gel column chromatography (EtOAc) to give **29** as a colorless oil (2.22 g, 94%). TLC (EtOAc) R_f 0.16. ^1H NMR (CDCl_3 , 200 MHz): δ 7.14–7.42 (m, 15 H), 3.55–3.69 (m, 26 H), 3.20 (t, $J = 4.9$ Hz, 2 H). ^{13}C NMR (CDCl_3 , 50 MHz): δ 143.9, 128.5, 127.5, 126.7, 86.3, 72.4, 70.3, 70.1, 63.1, 61.3. MS (ESI-TOF, 80 eV) m/z 568.30 ($\text{C}_{33}\text{H}_{44}\text{O}_8$), 591.33 (M + Na) $^+$, 607.32 (M + K) $^+$.

22-Azido-1,1,1-triphenyl-2,5,8,11,14,17,20-heptaaxadocosane (30). Compound **29** was mesylated according to the method used for compound **28**. It was purified by silica gel column chromatography (EtOAc): 81%. TLC (EtOAc) R_f 0.28. ^1H NMR (CDCl_3 , 200 MHz): δ 7.19–7.47 (m, 15 H), 4.32 (t, $J = 5.1$ Hz, 2 H), 3.60–3.72 (m, 24 H), 3.23 (t, $J = 5.1$ Hz, 2 H), 3.00 (s, 3 H). ^{13}C NMR (CDCl_3 , 50 MHz): δ 143.9, 128.5, 127.5, 126.7, 86.3, 70.4, 69.1, 68.7, 63.1, 37.4. MS (ESI-TOF, 80 eV) m/z 646.28 ($\text{C}_{34}\text{H}_{46}\text{O}_{10}\text{S}$), 669.27 (M + Na) $^+$, 405.18 (M + H – PPh_3C) $^+$, 243.11 (PPh_3C) $^+$. Displacement of the mesyl group was achieved by adding NaN_3 (290 mg, 4.46 mmol) to a solution of **29** (1.92 g, 2.97 mmol) in CH_3CN (100 mL). The mixture was refluxed overnight and then evaporated. CH_2Cl_2 (100 mL) was added, and the organic layer was washed with H_2O (50 mL) and brine (50 mL), dried over MgSO_4 , filtered, and evaporated. The crude product was chromatographed on a silica gel column (EtOAc/heptane 6/4) R_f 0.15. ^1H NMR (CDCl_3 , 200 MHz): δ 7.21–7.49 (m, 15 H), 3.64–3.68 (m, 24 H), 3.35 (t, $J = 4.6$ Hz, 2 H), 3.24 (t, $J = 4.8$ Hz, 2 H). ^{13}C NMR (CDCl_3 , 50 MHz): δ 144.0, 128.6, 127.6, 126.8, 86.4, 70.5, 69.8, 63.2, 50.5. MS (ESI-TOF, 80 eV) m/z 593.31 ($\text{C}_{33}\text{H}_{43}\text{N}_3\text{O}_7$), 616.31 (M + Na) $^+$, 632.28 (M + K) $^+$, 243.12 (PPh_3C) $^+$.

20-Azido-3,6,9,12,15,18-hexaoxaicos-1-yl-methane Sulfonate (31). To the compound **30** (1.35 g, 2.28 mmol) in MeOH (50 mL) was added TsOH (0.43 g, 2.88 mmol). The mixture was refluxed for 2 h, then Na_2CO_3 (2 eq) was added, and stirring was continued for 5 min. The solvent was evaporated under reduced pressure, and EtOAc (50 mL) was added to the crude product. The precipitate was filtered off, and the filtrate concentrated under reduced pressure. CH_2Cl_2 (50 mL) and Et_3N (0.35 mL, 2.50 mmol) were added to the crude product followed by MsCl (0.2 mL, 2.50 mmol) at 0 °C. Stirring was carried on for 2 h at 0 °C and then overnight at room temperature. The precipitate was filtered off, and the crude product was purified by silica gel column chromatography (EtOAc) to give **31** as a colorless oil (0.82 g, 84%). TLC (EtOAc) R_f 0.19. ^1H NMR (CDCl_3 , 200 MHz): δ 4.20 (t, $J = 4.4$ Hz, 2 H), 3.47–3.67 (m, 24 H), 3.22 (t, $J = 4.5$ Hz, 2 H), 2.92 (s, 3H). ^{13}C NMR (CDCl_3 , 50 MHz): δ 69.9, 69.4, 69.0, 50.1, 37.1. MS (ESI-TOF, 80 eV) m/z 429.18 ($\text{C}_{15}\text{H}_{31}\text{N}_3\text{O}_9\text{S}$), 430.16 (M + H) $^+$, 452.14 (M + Na) $^+$.

N-(20-Azido-3,6,9,12,15,18-hexaoxaicos-1-yl)piperazine, TFA Salt (32). To a solution of **31** (400 mg, 0.93 mmol) in CH_3CN (20 mL), Et_3N (0.26 mL, 1.86 mmol) and *N*-Boc piperazine **8** (0.21 mmol, 1.12 mmol) were added. The mixture was refluxed for 24 h. The precipitate was filtered off, and the filtrate was evaporated and chromatographed on a silica gel column (EtOAc/MeOH 95/5). TLC (EtOAc/MeOH) R_f 0.2. ^1H NMR (CDCl_3 , 300 MHz): δ 3.80–3.96 (m, 4 H), 3.46–3.60 (m,

24 H), 3.27 (t, $J = 4.6$ Hz, 2 H), 2.61 (t, $J = 4.3$ Hz, 2 H), 2.02–2.19 (m, 4 H), 1.43 (s, 9 H). ^{13}C NMR (CDCl_3 , 75 MHz): δ 154.7, 79.5, 70.6, 70.5, 70.4, 70.2, 67.9, 66.1, 57.5, 54.3, 50.3, 44.1, 40.0, 28.4. MS (ESI-TOF, 80 eV) m/z 520.31 (M + H) $^+$. The obtained Boc intermediate was then submitted to TFA (10 mL) deprotection for 2 h. The excess TFA was removed under reduced pressure, and the resulting compound was triturated in diethyl ether to give the expected product **32** in a 98% yield. ^1H NMR (CDCl_3 , 200 MHz): δ 5.60 (br s, 1 H), 3.81–3.94 (m, 4 H), 3.42–3.61 (m, 24 H), 3.26 (t, $J = 4.55$ Hz, 2 H), 2.64 (t, $J = 4.25$ Hz, 2 H), 2.01–2.15 (m, 4 H). ^{13}C NMR (CDCl_3 , 50 MHz): δ 79.4, 70.8, 70.5, 70.3, 70.2, 67.8, 66.0, 57.6, 54.7, 49.8, 43.0, 38.8, 28.2. MS (ESI-TOF, 80 eV) m/z 419.27 ($\text{C}_{18}\text{H}_{37}\text{N}_5\text{O}_6$), 420.21 (M + H) $^+$.

6-Amino-hexanoic Acid (4-[4-[2-Oxo-2-(6-oxo-5,6-dihydro-benzo[ϵ]pyrido[3,2-b][1,4]diazepin-11-yl)ethyl]piperazin-1-yl]butyl)amide (33). To a solution of **15** (142.7 mg, 0.40 mmol) in a mixture of dry DMF/DMSO (1/1), compound **6** (40 mg, 0.14 mmol) and DIPEA (0.15 mL, 0.84 mmol) were added. The mixture was heated at 80 °C for 10 h and then poured into brine and extracted with EtOAc. The organic layer was dried over Na_2SO_4 , filtered, and evaporated. The purity was checked by HPLC ($t_R = 31.12$ min.). MS (ESI-TOF, 135 eV) m/z 652.30 (M + H) $^+$, 674.30 (M + H) $^+$. The phthalimide protecting group was removed in an ethanolic solution of hydrazine (see procedure for compound **11**), and compound **33** was obtained in 80% yield as a white solid after purification by HPLC ($t_R = 22.96$ min.). ^1H NMR [(CD_3) $_2\text{SO}$, 300 MHz]: δ 8.22 (s, 1 H), 8.07 (d, 1 H, $J = 7.8$ Hz), 7.87 (m, 1 H), 7.64 (m, 3 H), 7.44 (m, 2 H), 3.64 (m, 2 H), 2.99 (m, 9 H), 2.88 (m, 2 H), 2.74 (t, 2 H, $J = 7.5$ Hz), 2.27 (s, 2 H), 2.06 (t, 2 H, $J = 7.2$ Hz), 1.16–1.60 (m, 14 H). ^{13}C NMR [(CD_3) $_2\text{SO}$, 75 MHz]: δ 172.3, 169.7, 166.8, 155.3, 144.4, 140.8, 133.2, 131.6, 131.1, 130.7, 130.0, 127.9, 125.7, 124.6, 61.3, 57.6, 52.5, 45.9, 39.2, 38.9, 35.7, 27.6, 27.3, 26.1, 25.4, 24.1. MS (ESI-TOF, 135 eV) m/z 521.31 ($\text{C}_{28}\text{H}_{39}\text{N}_7\text{O}_3$), 522.28 (M + H) $^+$.

6-Amino-hexanoic Acid [5-(4-[4-[2-Oxo-2-(6-oxo-5,6-dihydro-benzo[ϵ]pyrido[3,2-b][1,4]diazepin-11-yl)ethyl]piperazin-1-yl]butylcarbamoyl)pentyl]amide (34). Compound **34** was obtained according to the experimental conditions for compound **33** starting from **17** (14.4 mg, 0.028 mmol), **6** (4 mg, 0.014 mmol), and DIPEA (0.015 mL, 0.084 mmol) in a 1/1 mixture of DMF/DMSO. The mixture was heated at 80 °C for 10 h and then poured into brine and extracted with EtOAc. The organic layer was dried over Na_2SO_4 , filtered, and evaporated. The purity was checked by HPLC ($t_R = 34.4$ min.). MS (ESI-TOF, 135 eV) m/z 765.40 (M + H) $^+$, 787.41 (M + Na) $^+$. The phthalimide protecting group was removed in an ethanolic solution of hydrazine (see procedure for compound **11**), and the expected product **34** was purified by HPLC ($t_R = 23.56$ min.). Yield: 40%. ^1H NMR [(CD_3) $_2\text{SO}$, 200 MHz]: δ 8.26 (s, 1 H), 8.02 (d, 1H, $J = 7.7$ Hz), 7.86 (m, 1 H), 7.61 (m, 3 H), 7.44 (m, 2 H), 3.65 (m, 2 H), 2.92 (m, 8 H), 2.89 (m, 2 H), 2.74 (t, 2 H, $J = 7.5$ Hz), 2.26 (s, 2 H), 2.01 (t, 2 H, $J = 7.1$ Hz), 1.14–1.51 (m, 24 H). ^{13}C NMR [(CD_3) $_2\text{SO}$, 50 MHz]: δ 172.3, 169.5, 168.2, 166.9, 155.1, 143.9, 140.6, 132.8, 131.3, 131.0, 130.8, 130.5, 128.5, 125.2, 122.9, 65.3, 58.6, 53.2, 45.8, 44.2, 41.6, 39.1, 38.2, 35.7, 28.0, 27.1, 26.5, 26.0, 24.2. MS (ESI-TOF, 135 eV) m/z 634.40 ($\text{C}_{34}\text{H}_{50}\text{N}_8\text{O}_4$), 635.39 (M + H) $^+$.

11-[4-(2-Aminoethyl)piperazin-1-yl]acetyl]-5,11-dihydro-6H-pyrido[2,3b][1,4]benzodiazepin-6-one (35). Compound **21** (304 mg, 1.96 mmol) was dissolved in CH_3CN (20 mL), and Et_3N (0.41 mL, 2.94 mmol) and **6** (650 mg, 1.96 mmol) were added. The mixture was refluxed for 3 h. The solvents were evaporated, and the crude product was purified by silica gel column chromatography (EtOAc/MeOH 9/1, R_f 0.12), giving a colorless solid (397 mg, 50%). ^1H NMR (CDCl_3 , 200 MHz): δ 10.87 (br s, 1 H), 8.25 (s, 1 H), 7.93 (d, $J = 7.1$ Hz, 1 H), 7.59–7.68 (m, 3 H), 7.25–7.31 (m, 2 H), 3.31–3.62 (m, 4 H), 1.97–2.81 (m, 10 H). ^{13}C NMR (CDCl_3 , 50 MHz): δ 169.6, 168.7, 147.3, 144.7, 140.8, 133.4, 131.0, 130.7, 130.1, 128.7, 128.3, 127.9, 123.8, 60.9, 56.9, 56.7, 52.8, 52.6, 52.4, 48.0, 47.7, 29.5, 29.1. MS (ESI-TOF, 135 eV) m/z 407.19 ($\text{C}_{20}\text{H}_{23}\text{N}_8\text{O}_2$), 407.23 (M + H) $^+$, 813.41 (2M + H) $^+$.

To a solution of this azido-protected intermediate (200 mg, 0.49 mmol) in THF (10 mL) were added H₂O (14 μ L, 0.74 mmol) and PPh₃ (194 mg, 0.74 mmol). Stirring was pursued for 12 h at room temperature. The product was then purified by silica gel flash column chromatography (EtOAc to EtOAc/MeOH/Et₃N 89/10/1) to give the desired product **35** (150 mg, 80%). ¹H NMR (CDCl₃, 200 MHz): δ 8.34 (d, J = 3.4 Hz, 1 H), 8.02 (d, J = 7.6 Hz, 1 H), 7.35–7.80 (m, 8 H), 6.16 (br s, 2 H), 3.70 (m, 2 H), 3.43 (m, 2 H), 2.02–2.82 (m, 10 H). ¹³C NMR (CDCl₃, 50 MHz): δ 169.8, 168.3, 144.6, 140.7, 133.3, 131.9, 131.1, 130.2, 128.6, 123.9, 127.9, 61.0, 57.8, 52.3, 37.3. MS (ESI-TOF, 135 eV) m/z 381.20 (C₂₀H₂₅N₆O₂), 381.22 (M + H)⁺.

11-[(4-{2-[2-(2-Aminoethoxy)ethoxy]ethyl}piperazine-1-yl)acetyl]-5,11-dihydro-6H-pyrido[2,3-b][1,4]benzodiazepin-6-one (36). To a solution of **26** (152 mg, 0.626 mmol) in dry MeCN (25 mL) were added K₂CO₃ (238 mg, 1.72 mmol) and benzodiazepinone **6** (180 mg, 0.626 mmol). The mixture was refluxed for 20 h. The precipitate was collected by filtration and washed with CH₃CN, the filtrate was concentrated, and the crude product was purified by silica gel column chromatography (EtOAc/MeOH 9/1) to give the expected product (250 mg, 82%). TLC (EtOAc/MeOH 85/15) R_f 0.17. ¹H NMR (CDCl₃, 300 MHz): δ 10.53 (br s, 1 H), 8.22 (s, 1 H), 7.90 (d, J = 7.5 Hz, 1 H), 7.26–7.63 (m, 4 H), 3.13–3.60 (m, 12 H), 2.18–2.60 (m, 10 H). ¹³C NMR (CDCl₃, 75 MHz): δ 169.6, 168.3, 144.6, 140.7, 133.2, 131.0, 130.7, 130.1, 128.5, 127.9, 123.8, 70.4, 70.1, 69.8, 68.6, 68.0, 57.3, 52.9, 52.4, 50.5, 38.6, 30.2, 29.5. MS (ESI-TOF, 80 eV) 494.24 (C₂₄H₃₀N₈O₄), 495.26 (M + H)⁺.

To a solution of the azido-protected compound (250 mg, 0.506 mmol) in THF (50 mL), PPh₃ (200 mg, 0.76 mmol) and H₂O (14 μ L, 0.76 mmol) were added, and the mixture was stirred for 12 h. The solvents were then evaporated, and the crude product was chromatographed on a silica gel column with EtOAc until elimination of PPh₃ and OPPh₃, and then with EtOAc/MeOH/Et₃N (88/10/2) to EtOAc/MeOH/NH₄OH (85/10/5) to give product **36** (250 mg, 98%). TLC (EtOAc/MeOH/NEt₃ 88/10/2) R_f 0.07. ¹H NMR (CDCl₃, 300 MHz): δ 8.16 (br s, 1 H), 7.85 (d, J = 7.8 Hz, 1 H), 7.41–7.63 (m, 3 H), 7.17–7.33 (m, 2 H), 4.62 (br s, 2 H), 3.40–3.52 (m, 10 H), 2.80 (t, J = 5.2 Hz, 2 H), 1.94–2.51 (m, 10 H). ¹³C NMR (CDCl₃, 75 MHz): δ 169.5, 167.9, 144.2, 140.5, 132.9, 130.8, 130.6, 129.8, 128.5, 128.3, 127.7, 123.6, 76.6, 72.4, 69.9, 69.8, 68.7, 61.0, 57.3, 52.8, 52.4, 41.1. MS (ESI-TOF, 140 eV) m/z 468.24 (C₂₄H₃₂N₆O₄), 469.26 (M + H)⁺.

11-[(4-(20-Amino-3,6,9,12,15,18-hexaoxacos-1-yl)piperazin-yl)acetyl]-5,11-dihydro-6H-pyrido[2,3-b][1,4]benzodiazepin-6-one (37). Compound **32** (394 mg, 0.94 mmol) was dissolved in CH₃CN (20 mL). Then, Et₃N (0.26 mL, 1.86 mmol) and product **6** (270 mg, 0.94 mmol) were added. The mixture was refluxed for 2 h, then evaporated, and purified by silica gel column chromatography (EtOAc/MeOH/NH₄OH 86/10/4) to give the azido-protected intermediate (600 mg, 96%) as a pale yellow solid. ¹H NMR (CDCl₃, 300 MHz): δ 10.49 (br s, 1 H), 8.22 (br s, 1 H), 7.91 (d, J = 7.8 Hz, 1 H), 7.24–7.65 (m, 5 H), 3.38–3.62 (m, 28 H), 3.31 (d, J = 5.0 Hz, 2 H), 2.16–2.42 (m, 8 H). ¹³C NMR (CDCl₃, 75 MHz): δ 169.5, 168.1, 147.1, 144.5, 140.6, 133.1, 130.9, 130.7, 130.0, 128.6, 128.4, 127.8, 123.7, 70.3, 70.0, 69.8, 68.3, 67.9, 60.9, 57.3, 52.8, 50.4, 38.9. MS (ESI-TOF, 135 eV) m/z 670.34 (C₃₂H₄₆N₈O₈), 671.38 (M + H)⁺.

This product (600 mg, 0.895 mmol) was dissolved in THF (20 mL), and PPh₃ (352 mg, 1.34 mmol) and H₂O (24 μ L, 1.34 mmol) were added. The mixture was stirred overnight at room temperature, then evaporated, and chromatographed on silica gel column eluted with CHCl₃/MeOH/NH₄OH (88/10/2) to afford **37** as a pale yellow hygroscopic solid (437 mg, 76%). ¹H NMR (CDCl₃, 300 MHz): δ 8.20 (br s, 1 H), 7.89 (d, J = 7.5 Hz, 1 H), 7.55–7.66 (m, 3 H), 7.34–7.37 (m, 1H), 7.22–7.26 (m, 1 H), 4.47 (br s, 1 H), 3.43–3.65 (m, 28 H), 2.86 (br s, 2 H), 2.14–2.42 (m, 10 H). ¹³C NMR (CDCl₃, 50 MHz): δ 167.9, 166.6, 147.2, 144.4, 140.6, 133.0, 131.0, 130.0, 128.7, 127.9, 123.7, 70.3, 70.1, 68.5, 61.0, 57.3, 52.9, 52.5. MS (ESI-TOF, 250 eV) m/z 644.35 (C₃₂H₄₈N₆O₈), 645.42 (M + H)⁺.

Preparation of the Pirenzepine Fluorescent Derivatives. The fluorescent pirenzepine derivatives were obtained by coupling the corresponding pirenzepine spacers (2 μ mol) dissolved in dry DMF (20 μ L) with succinimidyl esters (1 μ mol) of either Bodipy [558/568], Rhodamine Red-X [560/580], or Fluorolink Cy3 [550/570] in the presence of DIPEA (3 μ mol), in a final volume of 25–30 μ L. The mixture was kept at room temperature in the dark. The reaction was monitored by HPLC (with UV absorbance detected at 219 and 530 nm) and was stopped upon complete disappearance of the starting fluorophore reagent (usually after 1 h). The products were purified by HPLC using a Zorbax (Z5 C8-25F) column, equilibrated in solvent A (H₂O 90%/CH₃CN 10%/TFA 0.1%; v/v), and eluted with a linear gradient from 0 to 100% of solvent B (CH₃CN 90%/H₂O 10%/TFA 0.1%;v/v) in 40 min at a flow rate of 1 mL/min. Fractions containing the product of interest were pooled and concentrated in a Speed Vac Concentrator (ISS 100, Savant).

When submitted to analytical HPLC, using the same column and elution conditions as described above, all concentrated probes were found to elute as single and symmetrical peaks at retention time t_R given below for each compound. The purity of the ligands was further confirmed by performing a second analytical HPLC run on a Zorbax (Z5C8-25QS; 250 mm \times 4.6 mm) column, equilibrated in solvent A (H₂O 90%/CH₃CN 10%/HFBA 0.1%; v/v), and eluted with a linear gradient from 0 to 100% of solvent B (CH₃CN 90%/H₂O 10%/HFBA 0.1%; v/v) in 60 min at a flow rate of 1 mL/min. Again, all final compounds eluted as homogeneous single peaks. The identities of the compounds were further analyzed by MALDI-TOF.

3-((2Z)-2-[[1-(Difluoroboryl)-5-thien-2-yl-1H-pyrrol-2-yl]methylene]-2H-pyrrol-5-yl)-N-methylpropanamide (38). t_R = 29.3 min. MALDI-TOF m/z 359.1075 (C₁₇H₁₆BF₂N₃OS), 381.209 (M + Na)⁺.

6-[[3-[[1-(Difluoroboryl)-5-[(Z)-(5-thien-2-yl-2H-pyrrol-2-ylidene)methyl]-1H-pyrrol-2-yl]propanoyl]amino]-N-(4-{4-[2-oxo-2-(6-oxo-5,6-dihydro-11H-pyrido[2,3-b][1,4]benzodiazepin-11-yl]ethyl)piperazin-1-yl]butyl}hexanamide (39). t_R = 31.3 min. MALDI-TOF m/z 849.3768 (C₄₄H₅₀BF₂N₉O₄S), 850.625 (M + H)⁺; 872.581 (M + Na)⁺; 888.448 (M + K)⁺.

6-[[3-((2Z)-2-[[1-Difluoroboryl]-5-thien-2-yl-1H-pyrrol-2-yl]methylene)-2H-pyrrol-5-yl]propanoyl]amino]-N-(6-oxo-6-[[4-{4-[2-oxo-2-(6-oxo-5,6-dihydro-11H-pyrido[2,3-b][1,4]benzodiazepin-11-yl]ethyl)piperazin-1-yl]butyl]amino]hexyl]hexanamide (40). t_R = 33.5 min. MALDI-TOF m/z 962.4608 (C₅₀H₆₁BF₂N₁₀O₅S), 963.876 (M + H)⁺; 985.980 (M + Na)⁺; 1002.003 (M + K)⁺.

3-[[1-(Difluoroboryl)-5-[(Z)-(5-thien-2-yl-2H-pyrrol-2-ylidene)methyl]-1H-pyrrol-2-yl]-N-(2-{4-[2-oxo-2-(6-oxo-5,6-dihydro-11H-pyrido[2,3-b][1,4]benzodiazepin-11-yl]ethyl)piperazinyl-1-yl]ethyl}propionamide (41). t_R = 33.4 min. MALDI-TOF m/z 708.2614 (C₃₆H₃₅BF₂N₈O₃S), 709.332 (M + H)⁺.

3-[[1-(Difluoroboryl)-5-[(Z)-(5-thien-2-yl-2H-pyrrol-2-ylidene)methyl]-1H-pyrrol-2-yl]-N-(2-{2-[2-{4-[2-oxo-2-(6-oxo-5,6-dihydro-11H-pyrido[2,3-b][1,4]benzodiazepin-11-yl]ethyl)piperazinyl-1-yl]ethoxy}ethoxy)ethyl}propionamide (42). t_R = 35.3 min. MALDI-TOF m/z 796.3138 (C₄₀H₄₃BF₂N₈O₅S), 797.474 (M + H)⁺.

3-[[1-(Difluoroboryl)-5-[(Z)-(5-thien-2-yl-1H-pyrrol-2-ylidene)methyl]-1H-pyrrol-2-yl]-N-(20-{4-[2-oxo-2-(6-oxo-5,6-dihydro-11H-pyrido[2,3-b][1,4]benzodiazepin-11-yl]ethyl)piperazinyl-1-yl]-3,6,9,12,15,18-hexaoxacos-1-yl}propionamide (43). t_R = 35.4 min. MALDI-TOF m/z 972.4187 (C₄₈H₅₉BF₂N₈O₉S), 973.403 (M + H)⁺; 995.485 (M + Na)⁺; 1011.280 (M + K)⁺.

N-{6-Diethylamino)-9-[4-((6-oxo-6-((2-[2-(2-{4-[2-oxo-2-(6-oxo-5,6-dihydro-11H-pyrido[2,3-b][1,4]benzodiazepin-11-yl]ethyl)piperazin-1-yl]ethoxy)ethoxy)ethyl]amino)-hexyl]amino)sulfonyl]-2-sulfophenyl]-3H-xanthen-3-ylidene)-N-ethyl Ethanaminium (44). t_R = 37.7 min. ES m/z 1121.4714 (C₅₇H₇₁N₉O₁₁S₂), 1122.570 (M + H)⁺, 561.79 [(M + 2H)⁺]².

2-((1*E*,3*E*)-3-{3,3-Dimethyl-1-[6-oxo-6-({2-[2-(2-{4-[2-oxo-2-(6-oxo-5,6-dihydro-1*H*-pyrido[2,3-*b*][1,4]benzodiazepin-11-yl)ethyl]piperazin-1-yl)ethoxy]ethyl]amino}hexyl]-5-sulfo-1,3-dihydro-2*H*-indol-2-ylidene}prop-1-enyl)-1-ethyl-3,3-dimethyl-5-sulfo-3*H*-indolium (45). $t_R = 27.0$ min. MALDI-TOF m/z 1080.4449 ($C_{55}H_{68}N_8O_{11}S_2^+$), 1081.331 ($M + H$)⁺.

Construction and Expression of the Chimeric hM1 Receptor. EGFP, preceded by the $\alpha 7$ nicotinic signal peptide, was fused via a short linker (SDL sequence) to the hM1 receptor N terminus. The latter was truncated (M1 to P18 deletion) so that the connecting sequence between EGFP's last residue (I230) and the receptor TM1 first residue (P22) was reduced to a peptide stretch of six amino acids. This receptor construct, referred to as EGFP(Δ 17)hM1 chimera, was subcloned into the pCEP4 vector and stably expressed in HEK 293 cells as described.¹⁴

Radioligand Binding. [³H]QNB binding was performed at 37 °C (1 h) on intact cells and suspended in Hepes-BSA buffer (10 mM Hepes, 137.5 mM NaCl, 1.25 mM MgCl₂, 1.25 mM CaCl₂, 6 mM KCl, and 10 mM glucose, pH 7.4; supplemented with 0.1 mg/mL bovine serum albumin) as previously reported.⁴¹ Receptor quantitation and competition experiments were done at a fixed (250 pM) [³H]QNB concentration, in the absence or in the presence of the fluorescent ligands or of 2 μ M atropine to assess nonspecific binding. K_i values of competitors were calculated from IC₅₀ values corrected for the concentration and K_i value (50 pM) of [³H]QNB.¹⁴

Spectroscopy. UV-visible absorbance spectroscopy was done with a Cary 1E spectrophotometer (Varian). Fluorescence measurements were made using a SPEX Fluorolog 2 (Jobin Yvon Horiba) spectrofluorimeter equipped with a 450 W Xe lamp.

Real-Time Fluorescence Monitoring of Ligand-Receptor Interactions. Experiments were performed on EGFP-(Δ 17)hM1 expressing cells, suspended in Hepes-BSA buffer (10 mM Hepes, 137.5 mM NaCl, 1.25 mM MgCl₂, 1.25 mM CaCl₂, 6 mM KCl, and 10 mM glucose, pH 7.4; supplemented with 0.1 mg/mL bovine serum albumin), typically at 3×10^6 cells/mL, and placed in a 1 mL thermostated quartz cuvette with magnetic stirring. Time-based recordings of the fluorescence emitted at 510 nm (excitation set at 470 nm) were performed at 21 °C and sampled every 0.2–10 s, depending on experiments.

Fluorescence binding measurements were initiated by adding the fluorescent ligand (4 μ L of a 250-fold concentrated DMSO stock) to the 1 mL cell suspension. Occupancy curves were generated by plotting amplitudes for fluorescence extinction (in percent) at equilibrium as a function of ligand concentration. K_d values and maximal FRET amplitudes were calculated by fitting data to the empirical Hill equation derived for saturation.

Once the binding equilibrium was reached, dissociation started with the addition of 5 μ M atropine (alone or combined with brucine) and fluorescence was recorded with time until full recovery of EGFP emission at 510 nm. Dissociation traces were fit (without any constraints) according to a monoexponential decay of fluorescence, allowing the determination of off-rate constants. Data were analyzed using Kaleidagraph 3.08 (Synergy Software) software.

Estimation of Donor-Acceptor Distances. The distance R_0 (Förster radius) for 50% transfer efficiency E , typical for each donor (EGFP)-acceptor (ligand fluorophore) pair, was calculated from $R_0 = 9790 (\kappa^2 n^{-4} \Phi_D J)^{1/6}$.¹⁵

κ^2 , a geometric factor that accounts for the relative orientation in space of the donor emission and acceptor absorption transition dipoles,¹⁵ was taken to be 2/3 (unless otherwise stated). n , the refractive index of the medium, has been taken to be 1.4. The quantum yield Φ_D of the donor (0.66 for EGFP) was taken from the literature.⁴² J , the spectral overlap integral for the combined emission of EGFP and absorbance of each fluorophore species, was calculated as previously described.⁶

The distance R (Å) between the EGFP and the fluorophore moiety of bound ligands was calculated using Förster's²⁷

equation: $R = R_0(1/E - 1)^{1/6}$. The efficiency of fluorescence energy transfer (E) was defined as the fractional decrease in EGFP fluorescence due to ligand binding and was expressed by $E = 1 - F_{DA}/F_D$, where F_{DA} and F_D are the specific donor fluorescence emissions in the presence or the absence of saturating concentrations of ligand, respectively. The specific EGFP fluorescence in the absence (F_D) or the presence (F_{DA}) of ligand was determined by subtracting the autofluorescence of nontransfected HEK cells (in the absence or presence of ligand) from the total fluorescence of hM1 chimera expressing cells.

Acknowledgment. This work was supported by the Centre National de la Recherche Scientifique, the Institut National de la Santé et de la Recherche Médicale, the Université Louis Pasteur, the Ministère de l'Enseignement Supérieur et de la Recherche (fellowship to I.P.) and Hoechst-Marion-Roussel (fellowship to C.T.).

Supporting Information Available: A Table listing the formulas, molecular and isotopic weights, MALDI-TOF analysis results, and HPLC elution times for compounds **1** and **38–45**. This material is available free of charge via the Internet at <http://pubs.acs.org>.

References

- (1) Szollosi, J.; Damjanovich, S.; Matyus, L. Application of fluorescence resonance energy transfer in the clinical laboratory: Routine and research. *Cytometry* **1998**, *34*, 159–179.
- (2) Hovius, R.; Vallotton, P.; Wohland, T.; Vogel, H. Fluorescence techniques: Shedding light on ligand-receptor interactions. *Trends Pharmacol. Sci.* **2000**, *21*, 266–273.
- (3) Berger, W.; Prinz, H.; Striessnig, J.; Kang, H. C.; Haugland, R.; Glossmann, H. Complex molecular mechanism for dihydropyridine binding to L-type Ca(2+)-channels as revealed by fluorescence resonance energy transfer. *Biochemistry* **1994**, *33*, 11875–11883.
- (4) Turcatti, G.; Nemeth, K.; Edgerton, M. D.; Meseth, U.; Talabot, F.; Peitsch, M.; Knowles, J.; Vogel, H.; Chollet, A. Probing the structure and function of the tachykinin neurokinin-2 receptor through biosynthetic incorporation of fluorescent amino acids at specific sites. *J. Biol. Chem.* **1996**, *271*, 19991–19998.
- (5) Steenros, K.; Hurskainen, P.; Eriksson, S.; Hemmilä, I.; Blomberg, K.; Lindqvist, C. Homogeneous time-resolved IL-2-IL-2R α assay using fluorescence resonance energy transfer. *Cytokine* **1998**, *10*, 495–498.
- (6) Vollmer, J. Y.; Alix, P.; Chollet, A.; Takeda, K.; Galzi, J.-L. Subcellular compartmentalization of activation and desensitization of responses mediated by NK2 neurokinin receptors. *J. Biol. Chem.* **1999**, *274*, 37915–37922.
- (7) Palanché, T.; Ilien, B.; Zoffmann, S.; Reck, M.-P.; Bucher, B.; Edelstein, S. J.; Galzi, J.-L. The neurokinin A receptor activates calcium and cAMP responses through distinct conformational states. *J. Biol. Chem.* **2001**, *276*, 34853–34861.
- (8) Valenzuela-Fernandez, A.; Palanché, T.; Amara, A.; Magerus, A.; Altmeyer, R.; Delaunay, T.; Virelizier, J.-L.; Baleux, F.; Galzi, J.-L.; Arenzana-Seisdedos, F. Optimal inhibition of $\times 4$ HIV isolates by the CXCL chemokine stromal cell-derived factor 1 α requires interaction with cell surface heparan sulfate proteoglycans. *J. Biol. Chem.* **2001**, *276*, 26550–26558.
- (9) Lecat, S.; Bucher, B.; Mely, Y.; Galzi, J.-L. Mutations in the extracellular amino-terminal domain of the NK2 neurokinin receptor abolish cAMP signaling but preserve intracellular calcium responses. *J. Biol. Chem.* **2002**, *277*, 42034–42048.
- (10) Ripoll, C.; Rubio, E.; Soria, B. Anthrolycholine bromide: a fluorescent ligand for the muscarinic receptor. *Gen. Physiol. Biophys.* **1992**, *11*, 241–249.
- (11) Karton, Y.; Baumgold, J.; Handen, J. S.; Jacobson, K. A. Molecular probes for muscarinic receptors: Derivatives of the M1-antagonist telenezepine. *Bioconjugate Chem.* **1992**, *3*, 234–240.
- (12) Jacobson, K. A.; Fisher, B.; van Rhee, A. M. Molecular probes for muscarinic receptors: Functionalized congeners of selective muscarinic antagonists. *Life Sci.* **1995**, *56*, 823–830.
- (13) Wang, Y.; Gu, Q.; Mao, F.; Haugland, R. P.; Cynader, M. S. Activity-dependent expression and distribution of M1 muscarinic ACh receptors in visual cortex neuronal cultures. *J. Neurosci.* **1994**, *14*, 4147–4158.
- (14) Ilien, B.; Franchet, C.; Bernard, P.; Morisset, S.; Weill, C. O.; Bourguignon, J.-J.; Hibert, M.; Galzi, J.-L. Fluorescence resonance energy transfer to probe human M1 muscarinic receptor structure and drug binding properties. *J. Neurochem.* **2003**, *85*, 768–778.

- (15) Lakowicz, J. R. *Principles of Fluorescence Spectroscopy*; Kluwer Academic/Plenum Publishers: New York, 1999.
- (16) Jakubik, J.; Bacakova, L.; El-Fakahany, E. E.; Tucek, S. Positive cooperativity of acetylcholine and other agonists with allosteric ligands on muscarinic acetylcholine receptors. *Mol. Pharmacol.* **1997**, *52*, 172–179.
- (17) Lazareno, S.; Gharagozloo, P.; Kuonen, D.; Popham, A.; Birdsall, N. J. M. Subtype-selective positive cooperative interactions between brucine analogues and acetylcholine at muscarinic receptors: Radioligand binding studies. *Mol. Pharmacol.* **1998**, *53*, 573–589.
- (18) Karton, Y.; Bradbury, B. J.; Baumgold, J.; Paek, R.; Jacobson, K. A. Functionalized congener approach to muscarinic antagonists: Analogues of pirenzepine. *J. Med. Chem.* **1991**, *34*, 2133–2145.
- (19) Hamuro, Y.; Geib, S. J.; Hamilton, A. D. Novel folding patterns in a family of oligoanthranilamids: nonpeptide oligomers that form extended helical secondary structures. *J. Am. Chem. Soc.* **1997**, *119*, 10587–10593.
- (20) Hulinska, H.; Polivka, Z.; Jilek, J.; Sindelar, K.; Holubek, J.; Svatek, E.; Matoussova, O.; Budesinsky, M.; Frycova, H.; Protiva, M. Experimental antiulcer agents: *N*-substituted 2-(4-methyl-1-piperazinyl) acetamides as piperazine models and some related compounds. *Collect. Czech. Chem. Commun.* **1988**, *53*, 1820–1844.
- (21) Wolfe, J. P.; Tomori, H.; Sadighi, J. P.; Yin, J.; Buchwald, S. L. Simple efficient catalyst system for the palladium-catalyzed amination of aryl chlorides, bromides and triflates. *J. Org. Chem.* **2000**, *65*, 1158–1174.
- (22) Greene, R. N. 18-crown-6: A strong complexing agent for alkali metal cations. *Tetrahedron Lett.* **1972**, *13*, 1793–1796.
- (23) Järv, J.; Hedlund, B.; Bartfai, T. Isomerization of the muscarinic receptor-antagonist complex. *J. Biol. Chem.* **1979**, *254*, 5595–5598.
- (24) Luthin, G. R.; Wolfe, B. B. [³H]Pirenzepine and [³H]quinuclidinyl benzilate binding to brain muscarinic cholinergic receptors. Differences in measured receptor density are not explained by differences in receptor isomerization. *Mol. Pharmacol.* **1984**, *26*, 164–169.
- (25) Jakubik, J.; El-Fakahany, E. E.; Tucek, S. Evidence for a tandem two-site model of ligand binding to muscarinic acetylcholine receptors. *J. Biol. Chem.* **2000**, *275*, 18836–18844.
- (26) Richards, M. H. Commentary. Pharmacology and second messenger interactions of cloned muscarinic receptors. *Biochem. Pharmacol.* **1991**, *42*, 1645–1653.
- (27) Förster, T. Zwischenmolekulare energiewanderung und fluoreszenz. *Ann. Phys. (Leipzig)* **1948**, *2*, 55–75.
- (28) Bourdon, H.; Trumpp-Kallmeyer, S.; Schreuder, H.; Hoflack, J.; Hibert, M.; Wermuth, C. G. Modelling of the binding site of the human m1 muscarinic receptor: experimental validation and refinement. *J. Comput.-Aided Mol. Des.* **1997**, *11*, 317–332.
- (29) Christopoulos, A.; Lanzafame, A.; Mitchelson, F. Allosteric interactions at muscarinic cholinergic receptors. *Clin. Exp. Pharmacol. Physiol.* **1998**, *25*, 185–194.
- (30) Lazareno, S.; Birdsall, N. J. M. Detection, quantitation, and verification of allosteric interactions of agents with labeled and unlabeled ligands at G protein-coupled receptors: Interactions of strychnine and acetylcholine at muscarinic receptors. *Mol. Pharmacol.* **1995**, *48*, 362–378.
- (31) Tucek, S.; Proska, J. Allosteric modulation of muscarinic acetylcholine receptors. *TIPS* **1995**, *16*, 205–212.
- (32) Kostenis, E.; Mohr, K. Two-point-kinetic experiments to quantify allosteric effects on radioligand dissociation. *TIPS* **1996**, *17*, 280–283.
- (33) Lysikova, M.; Havlas, Z.; Tucek, S. Interactions between allosteric modulators and 4-DAMP and other antagonists at muscarinic receptors: Potential significance of the distance between the N and carbonyl C atoms in the molecules of antagonists. *Neurochem. Res.* **2001**, *26*, 383–394.
- (34) Tränkle, C.; Weyand, O.; Voigtländer, U.; Mynett, A.; Lazareno, S.; Birdsall, N. J. M.; Mohr, K. Interactions of orthosteric and allosteric ligands with [³H]dimethyl-W84 at the common allosteric site of muscarinic M2 receptors. *Mol. Pharmacol.* **2003**, *64*, 180–190.
- (35) Lazareno, S.; Popham, A.; Birdsall, N. J. M. Allosteric interactions of staurosporine and other indocarbazoles with *N*-[methyl-³H]scopolamine and acetylcholine at muscarinic receptor subtypes: Identification of a second allosteric site. *Mol. Pharmacol.* **2000**, *58*, 194–207.
- (36) Birdsall, N. J. M.; Lazareno, S.; Popham, A.; Saldanha, J. Multiple allosteric sites on muscarinic receptors. *Life Sci.* **2001**, *68*, 2517–2524.
- (37) Lazareno, S.; Popham, A.; Birdsall, N. J. M. Analogues of WIN 62,577 define a second allosteric site on muscarinic receptors. *Mol. Pharmacol.* **2002**, *62*, 1492–1505.
- (38) Hall, D. A. Modeling the functional effects of allosteric modulators at pharmacological receptors: An extension of the two-state model of receptor activation. *Mol. Pharmacol.* **2000**, *58*, 1412–1423.
- (39) Christopoulos, A.; Kenakin, T. G protein-coupled receptor allostery and complexing. *Pharmacol. Rev.* **2002**, *54*, 323–374.
- (40) Liégeois, J. F. F.; Bruhwylter, J.; Damas, J.; Nguyen, T. P.; Chleide, E. M. G.; Mercier, M. G. A.; Rogister, F. A.; Delarge, J. E. New pyridonezodiazepine derivatives as potential antipsychotics: synthesis and neurochemical study. *J. Med. Chem.* **1993**, *36*, 2107–2114.
- (41) Weill, C.; Galzi, J.-L.; Chasserot-Golaz, S.; Goeldner, M.; Ilien, B. Functional characterization and potential applications for enhanced green fluorescent protein- and epitope-fused human M1 muscarinic receptors. *J. Neurochem.* **1999**, *73*, 791–801.
- (42) Tsien, R. Y. The green fluorescent protein. *Annu. Rev. Biochem.* **1998**, *67*, 509–544.

JM040800A